HILGARDIA

A Journal of Agricultural Science Published by the California Agricultural Experiment Station

VOLUME 12 | MARCH, 1939 | NUMBER 6

CONTENTS

UNIVERSITY OF CALIFORNIA · BERKELEY, CALIFORNIA

H I L G A R D I A

A Journal of Agricultural Science Published by the California Agricultural Experiment Station

VOL. 12 MARCH, 1939 No. 6

WATER CONDUCTION FROM SHALLOW WATER TABLES[1, 2]

ROSS E. MOORE[3]

INTRODUCTION

THE PHENOMENON of the flow of liquids through porous mediums without the application of external force and without complete filling of the pores of the solid with liquid, has long been recognized and studied. It was early recognized that the forces involved are those of adhesion and cohesion, the same as those responsible for the action of liquids in capillary tubes. The term "capillarity" (*6, 17*)[4] has thus come to apply to the flow of liquids through porous mediums.

Many analyses (*28–31*) have been made for the purpose of evaluating the capillary forces acting in three-phase systems, such as is the case in moist soil, consisting of solid, liquid, and gas, by assuming spherical solid particles of uniform size and sequence of packing arrangement. While this assumption has presented concepts of value in comprehending the mechanism involved in capillary flow, the size and configuration of the solid and liquid phases are very complex in even the most idealized systems, and become indeterminate when applied to natural bodies such as soil.

The capillary potential concept, introduced by Buckingham (*6*) in 1907, assumed a capillary force field generated by the attraction of moist soil for water. He defined a capillary potential, the gradient of which is equal in magnitude to the capillary force. The introduction of the potential function gave rise to the study of soil-moisture as a dynamic system; but this method received no added impetus until 1922, when Gardner (*9*) and others showed that the capillary potential of Buckingham may be

[1] Received for publication June 8, 1938.

[2] Abridged from a thesis submitted in partial fulfillment of the requirements for the degree of doctor of philosophy.

[3] Instructor in Soil Technology and Junior Soil Technologist in the Experiment Station.

[4] Italic figures in parentheses refer to "Literature Cited" at end of this paper.

considered as a pressure potential due to the differential pressures on either side of the liquid-gas interface in the menisci of the water films. They further showed it to be directly measurable, over a certain range of potential, by measuring the negative hydrostatic pressures within the water films of soil moisture. The instrument used for these direct measurements was called a capillary potentiometer, but is now called a tensiometer (*19*), and consists of a porous absorbing element, an adaptation of the Livingston Auto Irrigator, to which a manometer is attached. When the capillary potentiometer was filled with water and the porous absorbing element was embedded in the moist soil whose capillary potential was to be measured, water transfer took place between the porous element and the soil until, at equilibrium, the pressure of the water inside the potentiometer was equal to the pressure in the soil-moisture films. This pressure was read directly on the manometer.

In the application of the dynamic concept to soil moisture studies, the velocity of flow of water through the soil is considered to be proportional to the total water-moving force. A conductivity factor, variously called capillary conductivity, capillary transmission constant, conductivity, and permeability, has been used to express this proportionality (*3, 7, 8, 10, 16*). The term "permeability" is adopted in this paper.

Many data on the permeability of soils in saturated flow or, with the pore spaces entirely filled with water, are available in papers of the U. S. Geological Survey, the American Geophysical Union, and in engineering papers. Slichter (*24*) made theoretical calculations for the flow of underground water under pressure, in which it was assumed that the velocity of flow was proportional to the pressure gradient. There are relatively few published data on soil permeability in unsaturated flow, however. Such data as have been reported were derived from experimental results on relatively small quantities of soil through which flow was induced by artificially maintaining differential pressures in the moisture films on either side of the sample. Richards (*17, 18, 20*) has published data on three soils, including capillary potential as a function of water content, permeability as a function of water content and capillary potential, and permeability of a peat soil as a function of capillary potential.

The evaluation of the movement of water through unsaturated soil is important in many practical problems, such as: the drainage of land, of road subgrades, and of all structural foundations and pavements laid on the ground; the contribution of a water table to the water supply of plants; the loss of water from a soil surface by evaporation; and the upward translocation and concentration of soluble salts in the soil.

This paper reports pressure potential and saturated and unsaturated permeability data, using six California soils. The rate of water flow required to maintain shallow water tables in cylindrical soil columns 8 inches in diameter, was measured in graduated supply burettes. Unsaturated flow was induced naturally; the water rose from the water table to the surface of the soil columns by capillarity, and was evaporated from the surface. Tensiometers were spaced at regular intervals on the vertical axis of the soil columns, and the pressure potential values were read directly on these instruments. When the rate of water uptake and the pressure potentials throughout a soil column became steady, that column was said to be at steady state. Its moisture distribution was then determined by sampling, and its saturated and unsaturated permeabilities at various pressure potentials were determined from the velocity of flow and the total potential gradient.

PROCEDURE

The moisture studies reported herein were carried out in a room in a light frame building of the University of California at Berkeley. The room was 8×16 feet, and 12 feet high, with a reinforced concrete floor laid on the ground. The walls were of tongue-and-groove pine sheathing on 2×4 inch studs spaced at 2-foot centers, the naked studs being on the room side. After beginning this experiment, the walls and ceiling were lined with celotex wallboard which was nailed to the studs.

The room was heated by two batteries of electrical heating elements, one battery placed at either end of the room about 4 feet from the end walls and 6 feet from the floor. Heat distribution was effected by four electric fans, so placed as to give maximum air turbulence as well as general air circulation to all parts of the room.

The heating elements had two circuits, one continuous and one intermittent. The intermittent circuit was opened and closed by a thermal regulator through a relay. Temperature at the thermal regulator was set at 30° C, and controlled to about $\pm$ 0.02°. Temperature along the sides of the room and near the floor could not be held to this narrow range due to heat loss through the rather poorly insulated walls. The soil columns, which were set in a row close to a wall, normally held to a temperature range of 0.02° C, except during periods of abnormal change in the atmospheric temperature outside the room.

Six soils were used, ranging in texture from sand to clay (table 1). All except one, the Oakley sand, were of the Yolo series. The air-dry soils were prepared for filling the cans by breaking them down to pass a 3-mm screen.

The soil cans were of galvanized iron, cylindrical, 8 inches in diameter and 3 to 4 feet high (fig. 1), and were fitted with a wire-screen diaphragm soldered 2 inches above their bases to provide support for the soil columns. A water inlet tube, ¼ inch in diameter, was soldered 1 inch above the bottom of each can. Each can was punched with ⅝-inch holes in four vertical rows, one row at each quarter point on the can's circumference. The vertical distance between holes in the row and the elevation of each row, were arranged to give a hole for each inch of can height. Before a can was filled with soil the holes were closed with patches of

TABLE 1

Mechanical Analysis and Moisture Equivalents of the Soils Used

Separates	Oakley sand	Yolo sand	Yolo fine sandy loam	Yolo clay loam	Yolo light clay	Yolo clay
Fine gravel	0.2	2.9	0.1	0.1	....	....
Coarse sand	9.9	16.4	0.3	0.5	0.1	0.2
Medium sand	15.3	25.8	0.5	0.6	0.4	0.3
Fine sand	45.1	41.8	18.9	5.3	7.2	3.0
Very fine sand	20.4	6.0	31.0	21.0	16.1	8.1
Total sand	90.9	92.9	50.8	27.5	23.8	11.6
Total silt (by difference)	3.5	3.3	31.5	46.0	45.0	46.5
Total clay	5.6	3.8	17.7	26.5	31.2	41.9
Clay <2 micron	4.6	3.2	12.8	17.2	23.2	33.1
Clay <1 micron	4.0	2.9	9.4	13.5	17.4	26.5
Moisture equivalent	4.3	3.5	18.1	22.5	25.0	26.3

celluloid cemented to the outside. When the wetting front in the soil column reached a hole, the celluloid patch was removed, the soil sampled for moisture content, and the hole reclosed with a rubber stopper.

The procedure in filling the can with soil was similar to the tremie method for placing concrete under water (*36*). A strong fiber tube, 4 inches in outside diameter, and 4 feet long, originally made for the packing and shipment of glass tubing, was used as a tremie.

The tremie tube, surmounted by a funnel, was placed upright in the soil can. One man kept the funnel and tremie full of soil and a second man operated the tremie, partly supported its weight, kept it vertical, and moved it with a rotary motion so that the tube described a circle, the diameter of which was equal to the diameter of the soil can. The bottom of the tube, resting lightly on the soil, passed over the entire area of the soil column at each revolution, and thus maintained a level and regular surface. Approximately eight revolutions of the tremie were required per inch of depth of soil column laid down.

The entire system, can, tremie, and soil, was weighed at intervals of approximately 4 inches in the soil-column height. For the height of soil at each 4-inch stage the mean of eight to ten measurements was taken; these measurements were made from the top of the can with a meter stick which was dropped vertically onto the soil through a distance of ap-

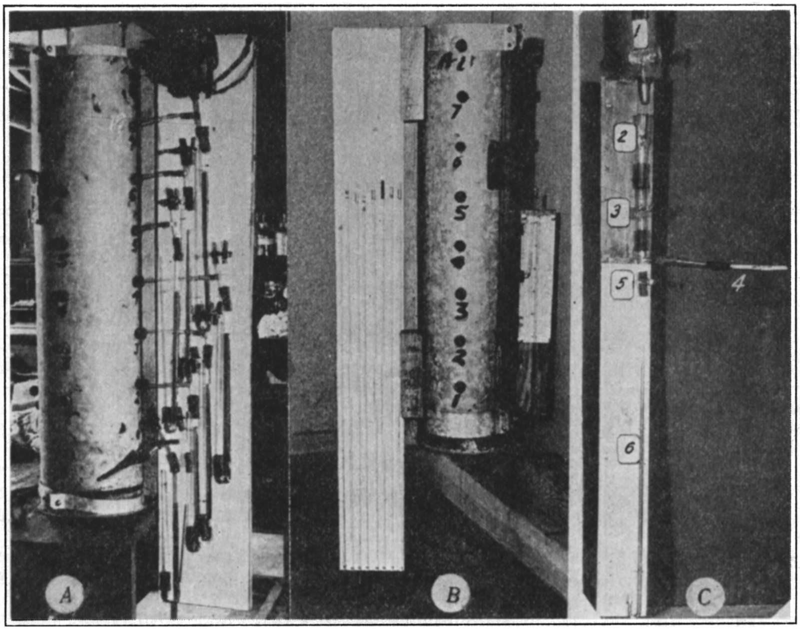

Fig. 1.—Soil cans with tensiometers installed.

A, Can with mercury tensiometers, showing the method of attaching the manometer panel and the installation of the tensiometers. The instrument at the top of the panel is a vibrator. The lowest tensiometer has been removed from the soil to show the cup (absorbing element).

B, Can with water tensiometers installed. Eight tensiometers with water manometers are mounted on the left panel. The tensiometers enter the soil column back of the panel. Two open water manometers used for positive potentials only are mounted on the small panel at the right.

C, Assembly of the tensiometer with a mercury manometer. This assembly was used for testing tensiometer cups and is the same as the tensiometers installed in the soil columns except that the stopcock, *3*, was replaced by a screw clamp. Details are as follows: *1*, A three-way stopcock sealed to a male standard taper ground glass connection. The two rubber tubing lines supply vacuum and water at atmospheric pressure. *2*, Female standard taper ground glass connection. *3*, Two-way stopcock. *4*, Porous fired-clay tensiometer cup. *5*, Screw clamp. *6*, Capillary staff of mercury manometer.

proximately 1 inch. The net weight of soil in the can was later corrected for air-dry water content.

Too few weighings were made on an individual soil column to allow a statistical calculation of variation in apparent density for a single column. A mean apparent density was calculated for each column, and the densities for each stage of filling were expressed as percentages of that mean. These percentages were collected for all the soil columns, analyzed statistically, and a single standard deviation was calculated and expressed as per cent variation from the mean apparent density. This single value was assumed to represent the standard deviation in apparent density for all the soil columns (table 2).

Water at constant pressure was supplied to the base of the columns by water supply units (fig. 2), carried upward through the soil by capillarity, and removed from the soil surface by evaporation. The rate at which water was taken up by the soil was measured in the graduated supply burettes of the water supply units, and the upward advance of the wetted front was observed through the celluloid-covered holes in the sides of the cans.

TABLE 2

CHARACTERISTICS OF THE SOIL COLUMNS

Soil type and can number	Length of soil column, centimeters	Cross section, square centimeters	Wetting time, days	Drying time, days	Mean apparent density	Standard deviation of apparent density	Standard deviation of mean apparent density	Per cent pore space	Per cent water at saturation by weight, oven-dry basis
Oakley sand, 3	117	314	312	9	1.48	0.042	0.004	43.3	29.2
Yolo sand, 13	84	322	108	5	1.49	.042	.005	43.0	28.8
Yolo fine sandy loam, 1	117	314	286	72	1.28	.036	.004	51.0	39.8
Yolo fine sandy loam, 17	84	322	21	7	1.24	.035	.004	52.5	42.3
Yolo fine sandy loam, 20	84	323	64	..	1.25	.035	.004	52.1	41.6
Yolo clay loam, 14	84	321	98	14	1.34	.038	.004	48.6	36.2
Yolo clay loam, 19	84	322	25	3	1.28	.036	.004	51.0	39.8
Yolo light clay, 2	117	314	310	34	1.32	.037	.004	49.5	37.5
Yolo light clay, 18	84	320	25	..	1.29	.036	.004	50.5	39.1
Yolo light clay, 20	84	323	29	3	1.27	.036	.004	51.3	40.4
Yolo clay, 15	84	322	89	13	1.28	.036	.004	51.0	39.8
Yolo clay, 16	84	312	37	..	1.22	0.034	0.004	53.2	43.5

Tensiometers (*19*), consisting of porous fired clay absorbing elements connected to vacuum gauges of the manometer type, were placed in the soil columns one above the other at intervals of 10 centimeters (fig. 1). A transfer of water takes place between the soil and the absorbing element until, at equilibrium, the pressure of the water in the absorbing element is equal to that in the moisture films of the soil. This pressure is calculated from the height of mercury or other manometer liquid used in the vacuum gauge.

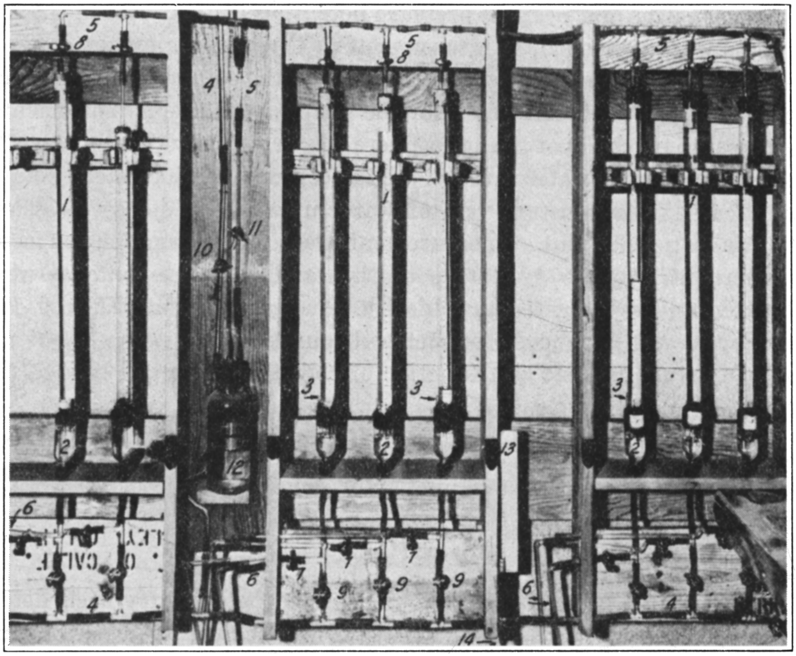

Fig. 2.—Battery of eight water supply units. The details are: *1,* Graduated burettes; *2,* constant-level reservoirs; *3,* air vents; *4,* water supply line from 20-liter supply bottle; *5,* suction line from 20-liter supply bottle; *6,* water lines from constant-level reservoirs to the soil columns; *7,* screw clamp cut-offs on water lines to the soil columns; *8,* screw clamp cut-offs on suction line; *9,* screw clamp cut-offs on water line from the 20-liter supply bottle; *10,* two-way stopcock on water line from 20-liter supply bottle; *11,* two-way stopcock on suction line from 20-liter supply bottle; *12,* water trap in the suction line; *13,* graduated staff tube for measurement of the outflow required to make burette, 1, "gurgle"; *14,* water outlet, used to drain water out of the system.

A burette was filled by closing *7* and opening *8* and *9*. By manipulating *10* and *11,* water flowed through *4* into the constant level reservoir, *2,* and was drawn up into the burette, *1,* by suction on the line, *5*. In operation, with water being supplied to the soil columns, *8* and *9* were closed and *7* was open. Two tubes ran through a 2-hole stopper from *1* into *2*. The lower ends of these tubes were at different elevations so that one tube was continuously immersed in water in *2,* and the end of the other controlled the variation in the elevation of the water level in *2*. When the water level dropped in *2,* air was admitted into *1* through the higher tube and water flowed from *1* to *2* through the other tube, raising the water level in *2* until the end of the higher tube was again immersed and the air supply to the burette was cut off. This cycle was called a "gurgle." At each "gurgle" about 6 cc of water flowed from *1* to *2,* causing a momentary rise of the water surface in *2* of about 0.5 cm. This was sufficient to cause a fluctuation of about 0.4 mm in the water table in the soil column, therefore a water table maintained by this method was relatively constant.

Both negative and positive pressure potentials of the water in the soil columns were measured with tensiometers. Open water manometers of the staff-gauge type were also used in some of the columns for the measurement of positive potentials. For the purpose of these measurements, the pressure potential of the atmosphere was arbitrarily taken as zero.

When the flow of water through the soil columns attained steady state, as indicated by a constant rate of water uptake and steady pressure potentials at each point of measurement, the soil was sampled for moisture content. The steady-state potentials and moisture contents were tabulated and represented graphically. The graphed data (figs. 9–13) include two wetting curves for each soil column:

(1) Moisture content as a function of elevation above the base of the soil,

$$P_w = f(H).$$

(2) Pressure potential as a function of elevation above the base of the soil,

$$\psi = F(H),$$

where: P_w is the per cent water in the soil on the oven-dry basis determined by drying for 24 hours at 105° C. H is the elevation in centimeters above the base of the soil column. ψ is the pressure potential in gram-centimeters per gram (in this paper abbreviated as gm–cm/gm).

After pressure potential and moisture content data had been collected for the soils wetting up, the water supply was removed and a soil-air interface was maintained at the base of the soil columns. During drying, the moisture density throughout the soil columns was reduced by continued evaporation from the surface and by downward flow of water. When the rate of moisture density change and pressure potential change had reached low values at all points in the soil columns, the soils were again sampled for moisture content and pressure potential readings were taken. These data were also tabulated and graphed as $P_w = f(H)$ and $\psi = F(H)$, drying.

The collection, tabulation, and graphical representation of all primary experimental data were included in the procedure outlined above. Later analysis of the primary data includes, first, an examination of the manner in which the pressure potential of a soil is affected by its moisture content, $\psi = f(P_w)$, and, second, an examination of the manner in which the soil permeability is affected by its pressure potential $K = F(\psi)$.

PRIMARY EXPERIMENTAL DATA

In this section are presented the quantitative experimental data discussed in the following order:

1. Mechanical analysis and moisture equivalent of the soils (table 1), and such characteristics of the soil columns as type, apparent density, and per cent pore space (table 2).

2. The manner in which pressure potentials and rate of water uptake vary with time during the wetting-up period (figs. 3 and 4).

3. The manner in which pressure potentials vary with time during the drying period (figs. 5 and 6).

4. The effect of temperature change on pressure potentials and the rate of water uptake in a soil column at steady state (fig. 8).

5. Pressure potentials and moisture distribution in soil columns at steady state (table 3 and figs. 9–13).

Soils Used.—The six soils used in the experiment were Oakley sand, Yolo sand, Yolo fine sandy loam, Yolo clay loam, Yolo light clay, and Yolo clay. All except the Yolo sand were collected from cultivated fields at depths of 2 to 8 inches. The Yolo sand is a stream-washed sand of the same origin as the Yolo soils and was collected in a commercial sand pit on the bank of Cache Creek.

The mechanical analysis of the soils was made by the pipette method using H_2O_2 and HCl pretreatment, and $Na_2C_2O_4$ as a dispersing agent.

The moisture equivalent determinations were made in duplicate on 30-gram samples of air-dry soil crushed to pass a 2-mm sieve. The samples weighed into the cups were moistened for 24 hours, drained for half an hour, and centrifuged for half an hour at a speed sufficient to develop a centrifugal force of 1,000 times gravity.

Mechanical analysis and moisture equivalent data are given in table 1. Numerical data descriptive of the soil in the columns are listed in table 2.

Pressure Potentials and Rate of Water Uptake as Functions of Time During the Wetting-Up Period.—The rate of water uptake as it decreased with time during approach to steady state was taken for all the soil columns. In figure 3 the log (rate of water uptake) is plotted as a function of the log (elapsed uptake time), $\log A = f(\log t)$, for Yolo clay, wetting. This curve is similar in form to those of all the soils studied in this experiment and conforms to observed data reported elsewhere (*35*) in the literature of which the example cited is only one of many.

An empirical equation for water uptake derived for a curve expressing

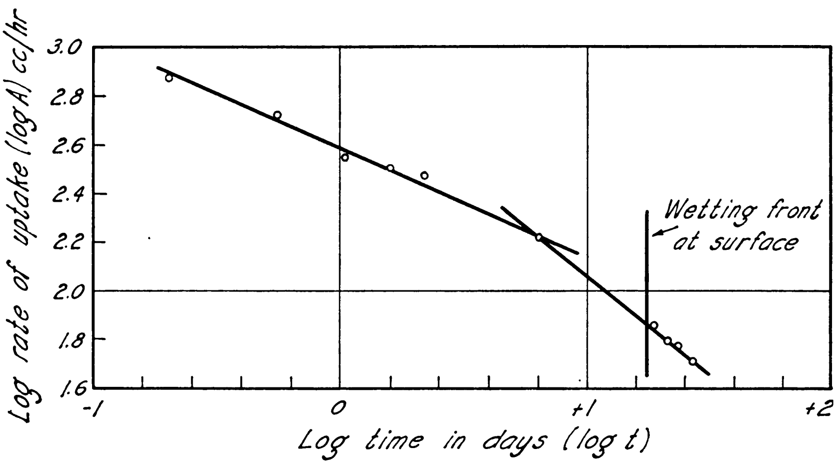

Fig. 3.—Rate of water uptake during approach to steady state, $\log A = f(\log t)$, for a column of Yolo clay wetting.

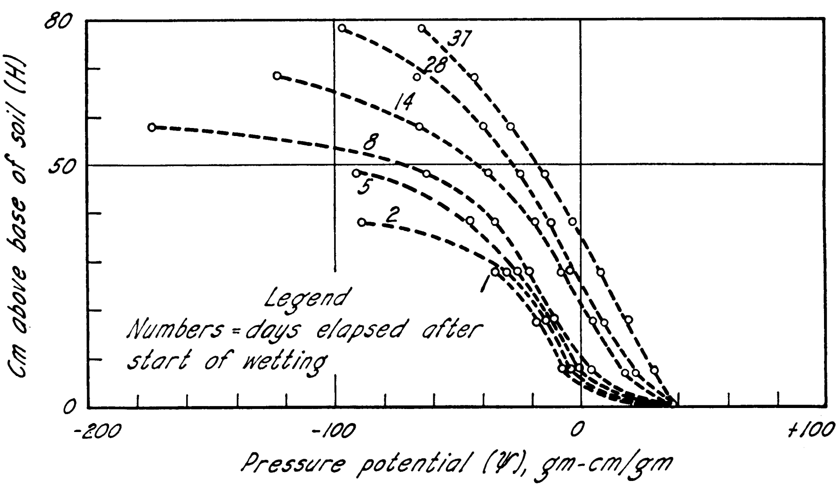

Fig. 4.—Distribution of pressure potential with the elevation above the base of the soil, $H = f(\psi)$ for a column of Yolo clay wetting.

$\log A = f(\log t)$ may be written in the form of an equation of a straight line,

$$\log A = -c(\log t) + \log K$$

or

$$A = kt^{-c}$$

where A is the rate of water uptake, t is the cumulative uptake time, and K and c are constants; c representing the slope or the rate of change of $\log A$ with $\log t$. The data for all the soil columns investigated conform to the first equation, with the exception that the value of c changed abruptly before the surface of the soil at the top of the columns had become obviously wet. Referring to figure 3, the initial stage of advance of the wetting front includes on the time scale, from inception of wetting to a log t in days of approximately 0.8 or an elapsed time of 6.3 days. During this time interval the wetting front advanced through air-dry soil of relatively constant apparent density and packing arrangement from near

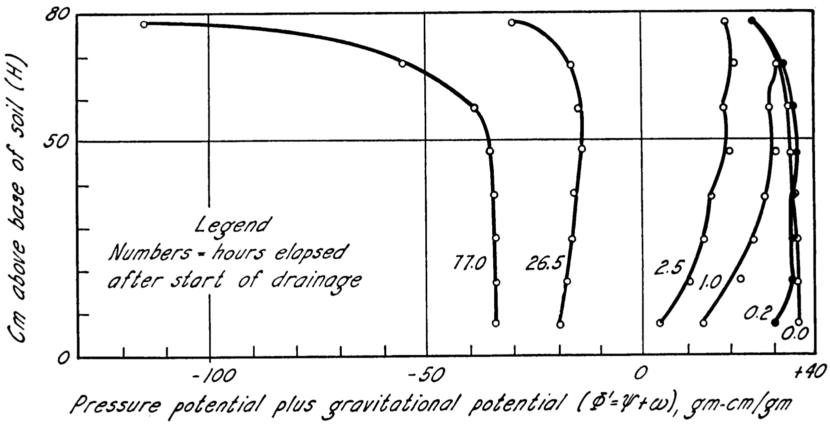

Fig. 5.—Distribution of the sum of the pressure and gravitational potentials with the elevation above the base of the soil, $H = f\,(\Phi')$ for a column of Yolo fine sandy loam drying.

the base of the soil column to within 1 or 2 mm of the surface. The 1 or 2 mm of soil at the top of the soil column was loosely packed and of lower apparent density than the remainder of the soil. Although the mulch was included in the length of the soil column, it is proposed that the contact between the mulch and the lower soil represented an irregular interface of discontinuity which was responsible for the change in the characteristic rate of water uptake.

A family of curves for Yolo clay representing the pressure potential distribution with elevation above the base of the soil at various cumulative wetting times is shown in figure 4, which, with the possible exception of the sands, is qualitatively characteristic of all the soils investigated during the wetting process. The potentials changed too rapidly in sands to be measured accurately.

Pressure Potential as a Function of Time During Drainage.—After upward flow in the soil columns had attained a steady state during the wetting process, the columns were drained by removing the water supply, and by maintaining a water-air interface at their bases. During drainage the change of pressure potential with time at various elevations in the soil columns was recorded. The rate of change of pressure potential varied with texture, being greatest for sand and least for clay. The general character of the drainage curves, however, was similar for all the soils; therefore, data are presented for one soil only.

Figures 5 and 6 represent pressure potentials during drainage of a 3-foot column of Yolo fine sandy loam which had come to a steady state

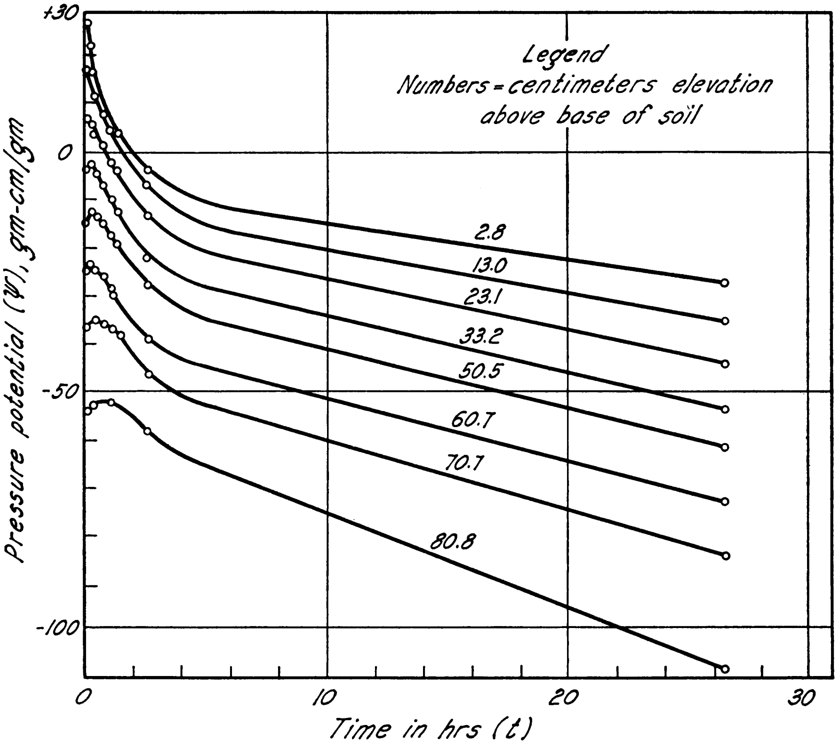

Fig. 6.—Distribution of the pressure potential at various elevations in the soil column with the time after drainage began, $\psi = f(t)$, in a column of Yolo fine sandy loam. Note the increase in pressure potentials in the unsaturated region of the column immediately after drainage began.

by wetting with a water pressure of 42 grams per square centimeter at the base of the soil column. The time when drainage began was arbitrarily taken as zero time, $t = 0$.

Figure 5 shows drainage curves for a column of Yolo fine sandy loam. For convenience in plotting, H is plotted as a function of Φ' which, however, should be considered the dependent variable, with the relation of Φ' to H expressed by the equation

$$\psi + \omega = \Phi' = f(H),$$

where H is the elevation above the base of the soil column in cm; ψ is the pressure potential in gm–cm/gm; ω is the gravitational potential in gm–cm/gm ($\omega = 0$ is arbitrarily taken at the elevation at which $\psi = 0$ when $t = 0$).

The total potential gradient had become approximately zero in the main body of the Yolo fine sandy loam column 60 hours after drainage began. This adjustment period required 24 hours and 96 hours in the Yolo sand and Yolo clay respectively.

Increases in pressure potentials immediately after drainage began were noted in all the cans at tensiometer positions above the water table (fig. 6). These increases indicated increases in the moisture density. Since even the highest tensiometer at an elevation of 80.8 cm above the base of the soil showed an increase in pressure potential, the water necessary must have been supplied from below.

A simple illustration taken from the case of a fully saturated single pore may explain the apparent anomaly of increasing pressure in the upper portion of a soil column induced by a sudden reduction in pressure at the base of the column. Figure 7 represents a capillary tube, the lower end of which had been dipped in water.

At time t_0 the water level has been lowered sufficiently to induce a temporarily reduced pressure potential about the lower tube opening, but at the same time to maintain a water connection between the free flat water surface and the capillary water in the tube. The pressure potential at the top of the capillary tube is ψ_0. Time t_0 represents the steady state condition in the soil columns at a position just above the surface of zero pressure potential.

At time t_1 the water level has been suddenly lowered. The water thread connecting the free flat water surface and the capillary water has broken. The water meniscus at the bottom of the capillary tube is convex to the air and the pressure immediately above the meniscus has increased from negative to positive.

At time t_2 the meniscus at the top of the capillary tube, which at t_0 was in equilibrium with a negative pressure at the base of the tube, has increased in radius of curvature to effect pressure equilibrium with the increased pressure at the base of the tube. An upward flow of water has taken place, and pressure potentials have increased throughout the capillary tube.

The discussion of the capillary tube in figure 7 deals with a fully saturated pore; whereas this experiment deals with a porous medium which is not saturated throughout its length, but is a three-phase system containing solid, liquid, and air. The energy involved, however, in the adjustment of water by capillarity in an unsaturated soil is due to the forces of gravity, adhesion, and cohesion, the same as are responsible for the movement of water in figure 7. The pressure potential changes induced by drainage of a soil column under the conditions of this experiment may be appropriately discussed by analogy to the capillary tube.

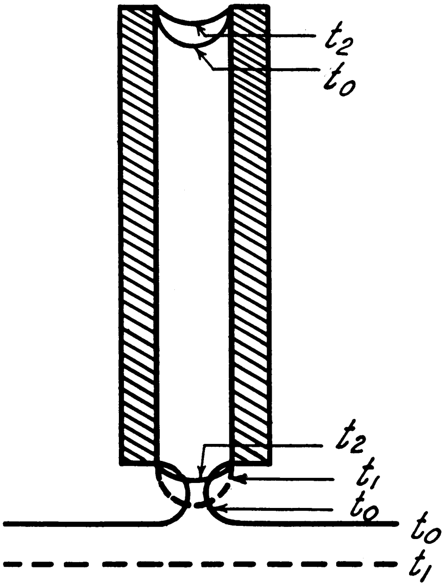

Time	Pressure in water under meniscus	
	Lower end	Upper end
t_0	−	−
t_1	+	
t_2	less +	less −

Fig. 7.—Diagrammatic illustration of the menisci and their changes in curvature during the withdrawal of a capillary tube from water.

The break in the continuity of the water system shown at time t_1 occurs in the large pores in the soil columns; the smaller moisture films in the soil which are capable of greater curvature remain continuous. Permeability in the moisture films of low curvature is relatively high; the pressure increase at the point of rupture of the large films postulated at a time corresponding to t_1 would result in an upward flow of water causing a temporary increase in pressure potentials.

General laboratory experiments on the distribution of water in soil over a water table have been conducted by setting soil tubes filled with soil in vessels of water (*14, 15, 23*). In this type of experiment the soil rests on a porus support near the bottom of the soil tube and is in contact with water at atmospheric pressure. The elevation of the water in the outer vessel is kept constant, and it is assumed in these cases that the water table in the soil is at this elevation. After a duration of time, assumed to be sufficient for the establishment of a steady moisture distribution in the soil columns, the tubes are removed from the vessels of water and are sampled for moisture content. Such laboratory experiments have generally shown the highest moisture content to be some distance above the original water table. This distribution has been so universally observed in experiments that the experimental results have been interpreted as representing the actual moisture distribution in an undisturbed soil over a water table.

It should be observed here that removing the soil tubes from the vessels of water is not essentially different from the drainage technique reported in this paper. Consequently, the changes in pressure potentials during drainage which were observed in the experiment reported herein must have also taken place in the experiments cited above. These pressure potential changes (fig. 6) indicate that an upward flow of water takes place immediately after drainage begins, which flow may cause the highest moisture content, at the time the column is sampled, to occur at some distance above the original water table.

Effect of Temperature Variation on Pressure Potentials and Rate of Water Uptake.—The experiment was designed to study soil-moisture movement at constant temperature. Temperature variation in the soil was held within a range of 0.2° C except during four short periods during which a high positive correlation between increasing or decreasing temperature and certain observed features in the behavior of the soil-moisture system permits a statement of the qualitative effect of temperature variation on these features.

A drop in temperature always resulted in an increased rate of water intake and in lower pressure potentials throughout the columns in all the soils. A rise in temperature had the reverse effects. A drop in temperature of 1° C in one hour lowered the water table 3 cm in the Yolo sand and 12 cm in the Yolo clay with intermediate amounts for soils of intermediate texture.

In the soil columns at steady state, with temperature constant, the soil-moisture system is in delicate balance, water flows through the column at a constant rate, and the pressure potentials throughout the soil mass are steady and dependent upon the permeability of the soil and the velocity of flow. The moisture gradient is fixed by the pressure potential

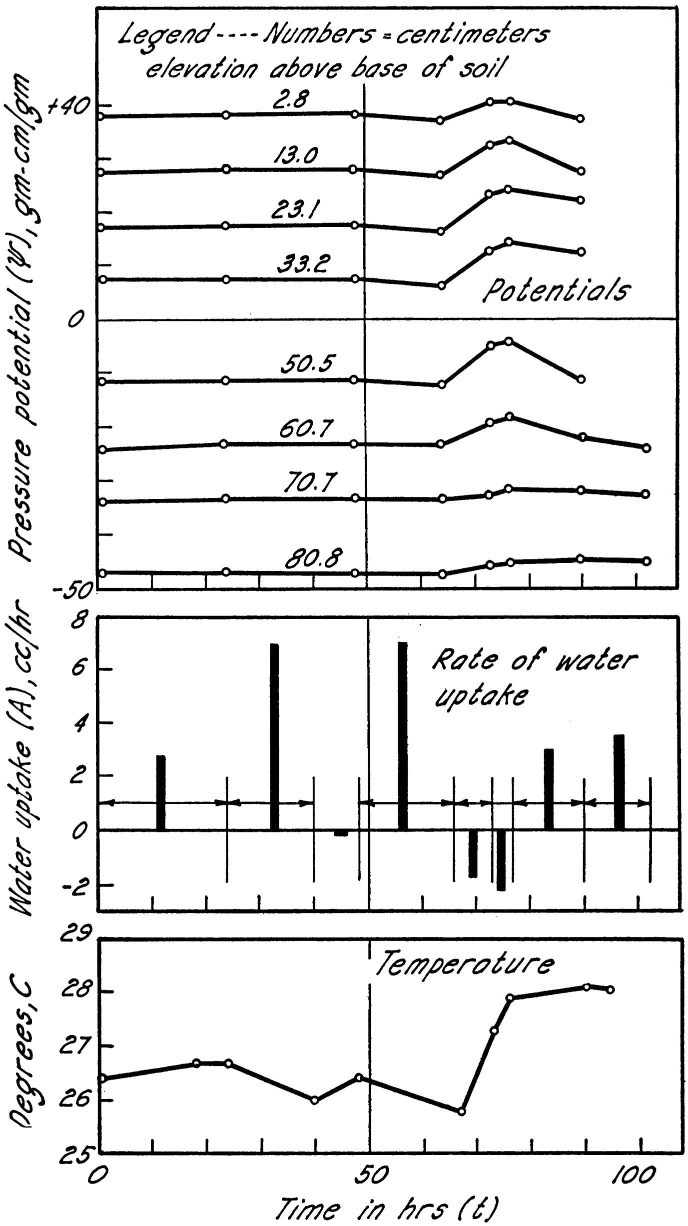

Fig. 8.—The effect of changes in temperature on pressure potentials and rate of water uptake in a column of Yolo fine sandy loam.

gradient, the displacement of which initiates adjustments in the soil-moisture density in the direction of re-establishment of the steady-state gradient.

Surface tension decreases and pressure potential in unsaturated soil increases with increasing temperature. Therefore, an unsaturated soil at a given potential holds less water at a higher than at a lower temperature. After a rise in temperature, water drains downward through the soil, gradually reducing the pressure potentials in the upper portion of the soil column and increasing still further the pressure potentials in the lower portion. During this phase of readjustment, temporary water tables were recorded up to 15 cm higher than the pressure head of the supply line. With decrease in temperature, the cycle described above is reversed; the pressure potentials become more negative, the rate of water uptake increases, and the water table drops.

The magnitude of the potential variations and changes in rate of water uptake with changes in temperature depend upon the rate of temperature change, the permeability of the soil, and the relation of pressure potential to moisture content. If the change in temperature is sufficiently slow or if the soil permeability is sufficiently high, redistribution of water in the soil may take place with sufficient rapidity to maintain relatively constant potentials, and the only obvious major deviation from steady state is the rate of water uptake.

The performance of a column of Yolo fine sandy loam during a period of temperature variation is shown graphically in figure 8. At zero time the pressure potentials in the soil column were at steady state with a rate of water uptake 3.9 cubic centimeters per hour, and a temperature (T) of 26.4° C. The graph may be divided into several time periods for the purpose of discussion:

1. $t = 0$ hours to $t = 24$ hours.
   A. $\Delta T/\Delta t = +0.013°$ C per hour.
   B. Small increase in pressure potentials.
   C. Decrease in rate of water uptake.

2. $t = 24$ hours to $t = 40$ hours.
   A. $\Delta T/\Delta t = -0.044°$ C per hour.
   B. No appreciable change in pressure potentials.
   C. Great increase in rate of water uptake.

3. $t = 40$ hours to $t = 48$ hours.
   A. $\Delta T/\Delta t = +0.05°$ C per hour.
   B. No significant change in pressure potentials.
   C. Rate of water uptake decreased to a negative value.

4. $t = 48$ hours to $t = 67$ hours.
   A. $\Delta T/\Delta t = -0.032°$ C per hour.
   B. Slight decrease in pressure potentials.
   C. Great increase in rate of water uptake.

5. $t = 67$ hours to $t = 76$ hours.
   A. $\Delta T/\Delta t = +0.23°$ C per hour.
   B. Increase in pressure potentials of 2 gm–cm/gm at 81 cm above the base of the soil column, and increasing progressively to more than 10 gm–cm/gm at the water table. Water flowed downward through the soil and out of the can via the supply line. Greater potentials would have been registered if water had not been lost from the system.
   C. The rate of water uptake became negative. The negative absorption rates shown on the graph do not represent the total amount of water drained out of the soil column. An undetermined amount of water was lost through the vent tube in the constant-level supply reservoir.

6. $t = 76$ hours to $t = 95$ hours.
   A. Temperature changing very slowly and approaching 28.2° C.
   B. Pressure potentials rapidly decreasing toward establishment of of a steady-state gradient approximately equivalent to that at $t = 0$.
   C. Rate of water uptake approaching the rate at the previous steady state.

It is evident that temperature variations may vitiate the accuracy of many types of soil-moisture studies. Fluctuations in soil moisture contents and water tables in field studies may be erroneously attributed to causes other than temperature unless the variations in temperature and their attendant effects are known (*25–27*). The quantitative evaluation of the various effects that temperature variations may have on the soil moisture system would constitute a major problem.

Pressure Potential and Moisture Distribution at Steady State.—Pressure potential and moisture content data in soil columns at steady state are tabulated in table 3, and are represented graphically in figures 9–13. The moisture samples were approximately 10-gram core samples taken with a thin-walled, polished, aluminum tube ½ inch in diameter which was thrust horizontally into the soil column through holes in the side of the soil can. The soil sample was quickly transferred to a weighing bottle by pushing the core out of the sampling tube with a tight-fitting plunger. A soil column was sampled, taking 16 samples, in about 3 minutes.

The tube method of sampling was satisfactory for moisture contents up to approximately 85 to 90 per cent of saturation, but beyond this moisture range very erratic results were secured. Great limitations were imposed on the possible methods for taking samples by the design of the

TABLE 3*

MOISTURE CONTENT AND PRESSURE POTENTIAL; EXPERIMENTAL VALUES FOR YOLO LIGHT CLAY, CAN NO. 2†

Elevation above water table	Wetting		Drying	
	Moisture content, P_w (oven-dry basis)	Pressure potential, ψ	Moisture content, P_w (oven-dry basis)	Pressure potential, ψ
cm	*per cent*	*gm-cm/gm*‡	*per cent*	*gm-cm/gm*
3.5	33.8	− 3.7	.....	− 11.0
8.7	36.0	....	34.92	....
13.9	34.1	− 15.1	.....	− 23.0
19.0	35.8	....	33.53	....
24.2	30.3	− 26.5	.....	− 34.3
29.0	33.8	....	30.58	....
34.1	30.0	− 39.6	.....	− 44.1
39.1	28.7	....	28.60	....
44.2	28.2	− 56.2	.....	− 62.8
49.4	28.0	....	27.55	....
54.6	26.8	− 75.8	.....	− 84.5
59.6	26.4	....	26.49	....
64.6	25.1	− 96.4	.....	−104.7
69.6	24.9	....	24.50	....
74.6	23.8	−134.9	.....	−135.0
79.7	23.4	....	23.15	....
84.8	22.3	−198.8	.....	−200.0
90.0	21.2	....	21.31	....
95.1	19.8	−359.5	.....	−377.6
100.1	....	−599.0	18.54	−610.0
105.1	{14.4 14.7}	....	....	....

* Plotted in figure 11.
† Owing to the limitations of space in this paper, tabular experimental data on the distribution of pressure potentials and moisture is given for one soil column only.
‡ Gm-cm/gm and gm/gm are used throughout this paper as units of work and of force respectively. These values may be multiplied by 980 to obtain dynes and ergs.

soil cans, and the necessity for a minimum disturbance of the soil and alteration of the cross section of the column. The tube method was used for all sampling.

The $P_w = f(H)$ curves (figs. 9–13) were plotted from the experimental data from the lower moisture contents up to 85 to 90 per cent of saturation, and projected from this point to saturation. Experimental values for moisture contents were disregarded in the wet portion of the curve. The zone of saturation was assumed to extend from the base of the soil through the region of positive pressure potentials, and to the

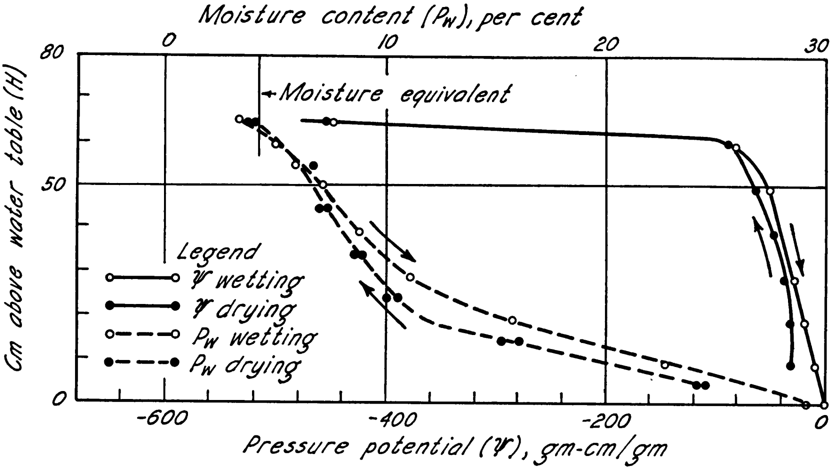

Fig. 9.—Curves of $P_w = f(H)$ and $\psi = F(H)$ for a column of Oakley sand at steady-state wetting and after drainage. For convenience in representation, P_w and ψ are plotted as abscissas.

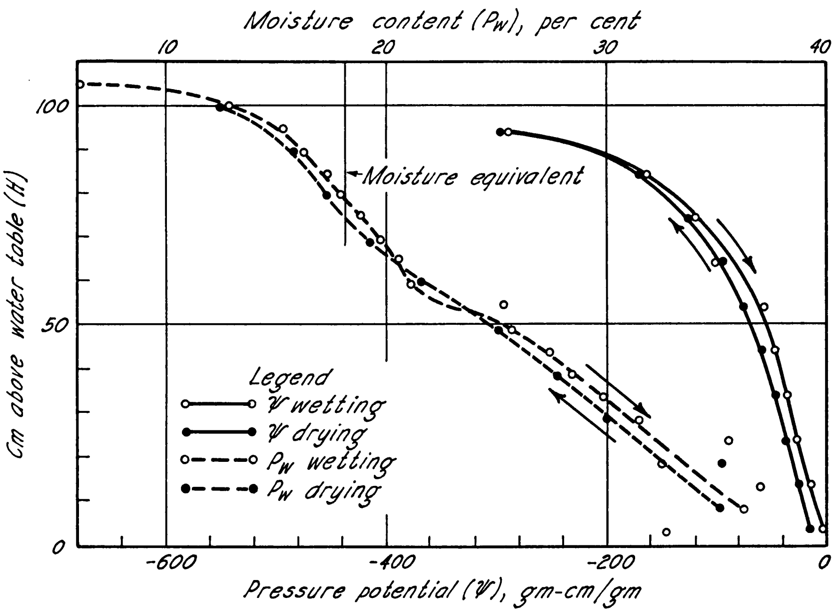

Fig. 10.—Curves of $P_w = f(H)$ and $\psi = F(H)$ for a column of Yolo fine sandy loam at steady-state wetting and after drainage. For convenience in representation, P_w and ψ are plotted as abscissas.

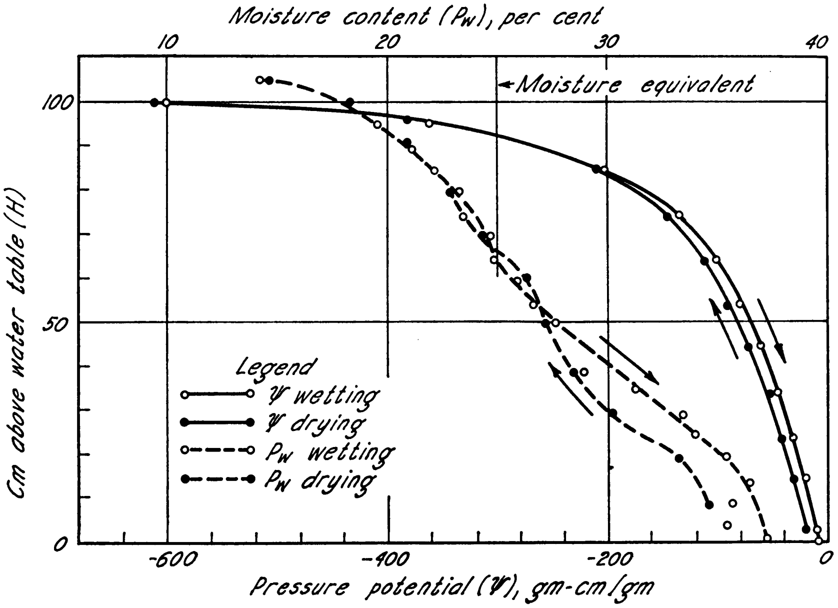

Fig. 11.—Curves of $P_w = f(H)$ and $\psi = F(H)$ for a column of Yolo light clay at steady-state wetting and after drainage. For convenience in representation, P_w and ψ are plotted as abscissas.

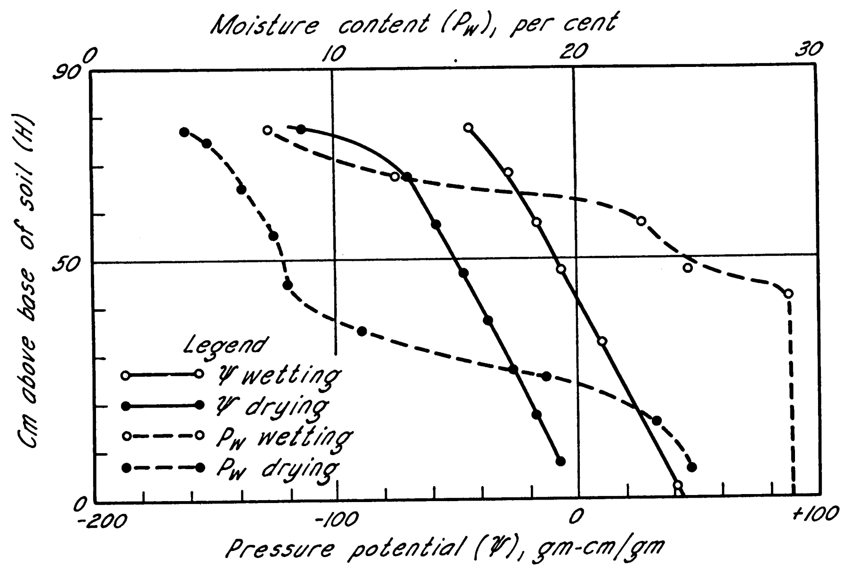

Fig. 12.—Curves of $P_w = f(H)$ and $\psi = F(H)$ for a column of Yolo sand at steady-state wetting and after drainage. For convenience in representation, P_w and ψ are plotted as abscissas.

elevation of zero pressure potential. The moisture content of the soil at saturation was calculated from the apparent density of the soil, assuming a real density of 2.61.

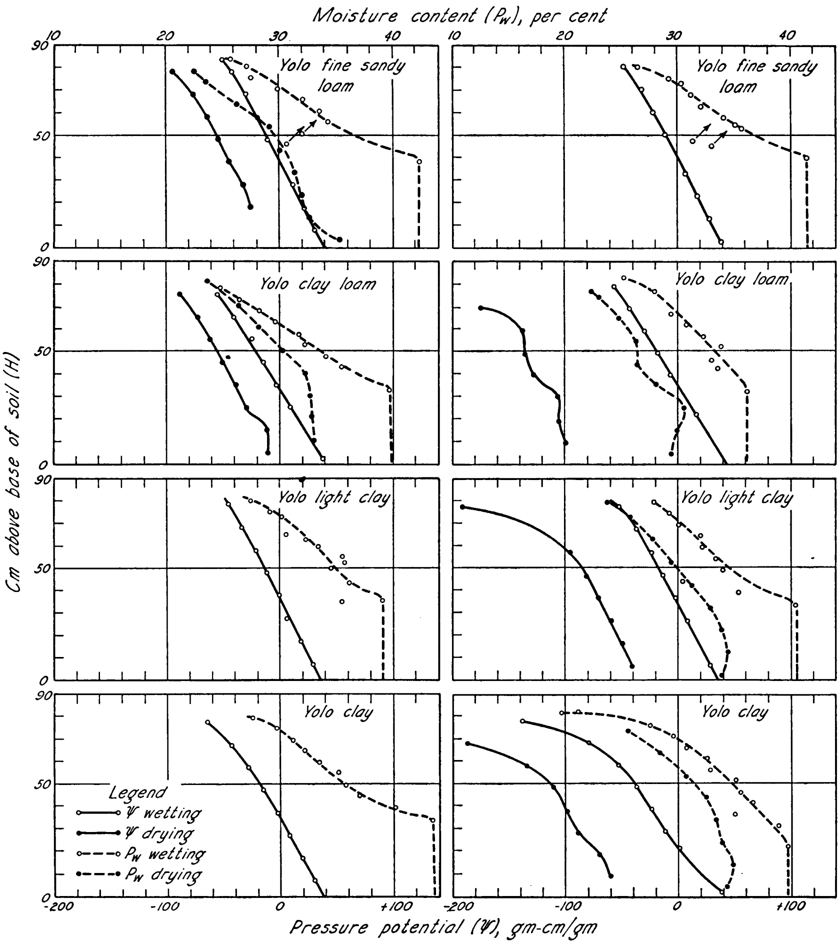

Fig. 13.—Curves of $P_w = f(H)$ and $\psi = F(H)$ for columns of soil at steady-state wetting and after drainage. For convenience in representation, P_w and ψ are plotted as abscissas.

ANALYSIS OF THE PRIMARY EXPERIMENTAL DATA

The Relation between Pressure Potential and Water Content of Soils at 29° C.—The relation between pressure potential, ψ, and moisture content, P_w, in each soil column is represented graphically in curves (figs. 14–18) of $\psi = f(P_w)$. These curves were developed for the soils at a steady state during the wetting process, and after drainage, from the primary moisture content and pressure potential data as expressed in curves of $P_w = f(H)$ and $\psi = F(H)$.

Differences in vapor pressure and pressure potentials for the same medium at the same moisture content, the magnitude of which depends

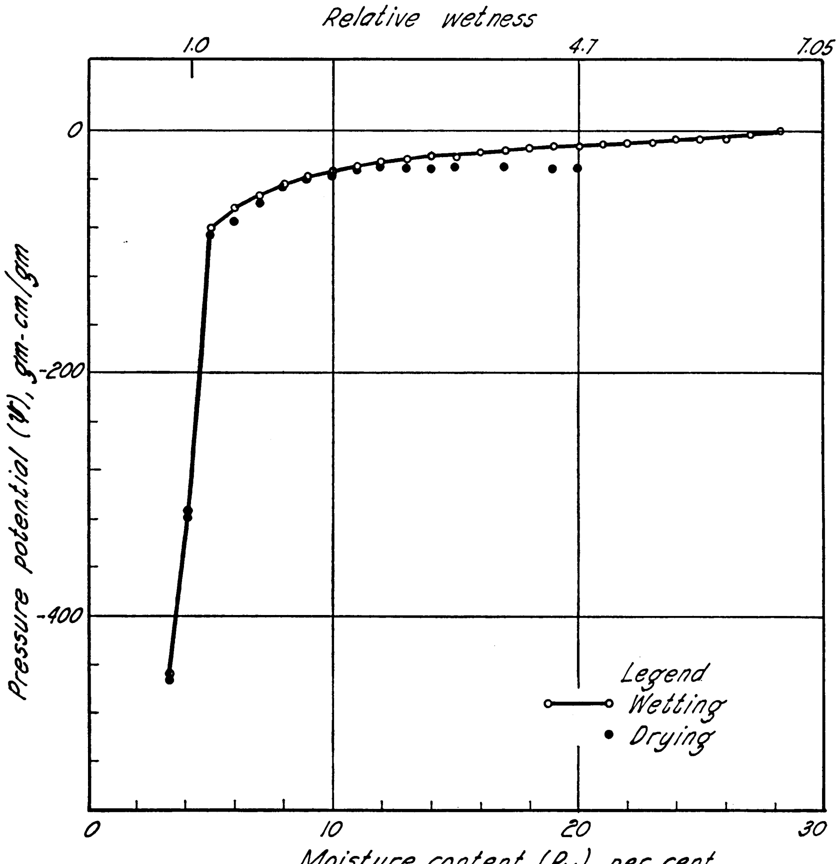

Fig. 14.—Curve of $\psi = f(P_w)$ for Oakley sand wetting and drying.

upon whether the medium is wetting or drying, have often been reported. This phenomenon has been referred to hysteresis effects (*11, 12, 21*), and has been reported in a wide variety of media (*32*) in which capillarity is active in the distribution and retention of liquids. Hysteresis has been attributed by the early workers to the alteration of the contact angle between solid and liquid due to adsorbed air on the solid. Adam (*1*) attributes the alteration of the contact angle to the frictional resistance between liquid and solid. Smith (*29, 30*) and his associates working with an "ideal soil" attribute maximum, minimum, and intermediate capillary rise to the cyclic alteration in pore cross section incident to any type of packing of spheres. Hysteresis is generally reported for wetting and

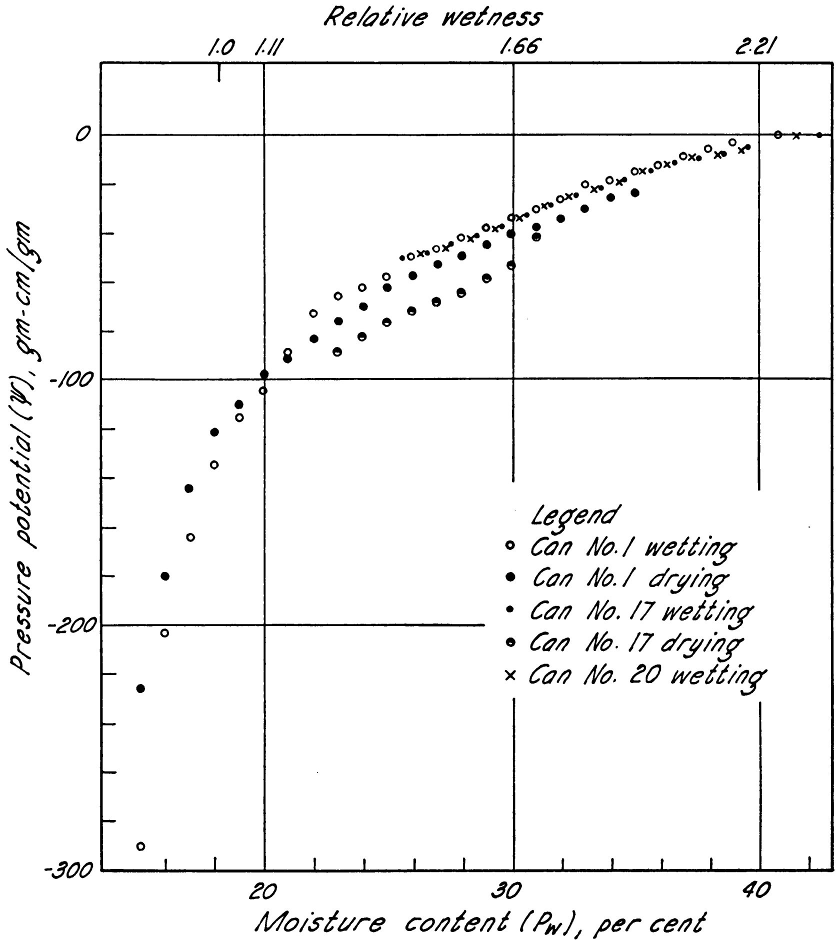

Fig. 15.—Curve of $\psi = f(P_w)$ for Yolo fine sandy loam wetting and drying.

drying clays, and for colloidal separates of clays dried or wetted in evacuated desiccators over osmotic solutions.

In the procedure followed in this experiment, drainage of the soil columns was accompanied by flow of water from the tensiometer cup to the soil, and by settlement and attendant increase in apparent density of the soil. A lag in pressure equilibrium between the tensiometer cup and the soil would have indicated an apparent hysteresis, but opposite in sign to that observed. At a given moisture content and increased apparent density, the negative radius of curvature would increase and the vapor pressure and the pressure potential should increase. Settlement

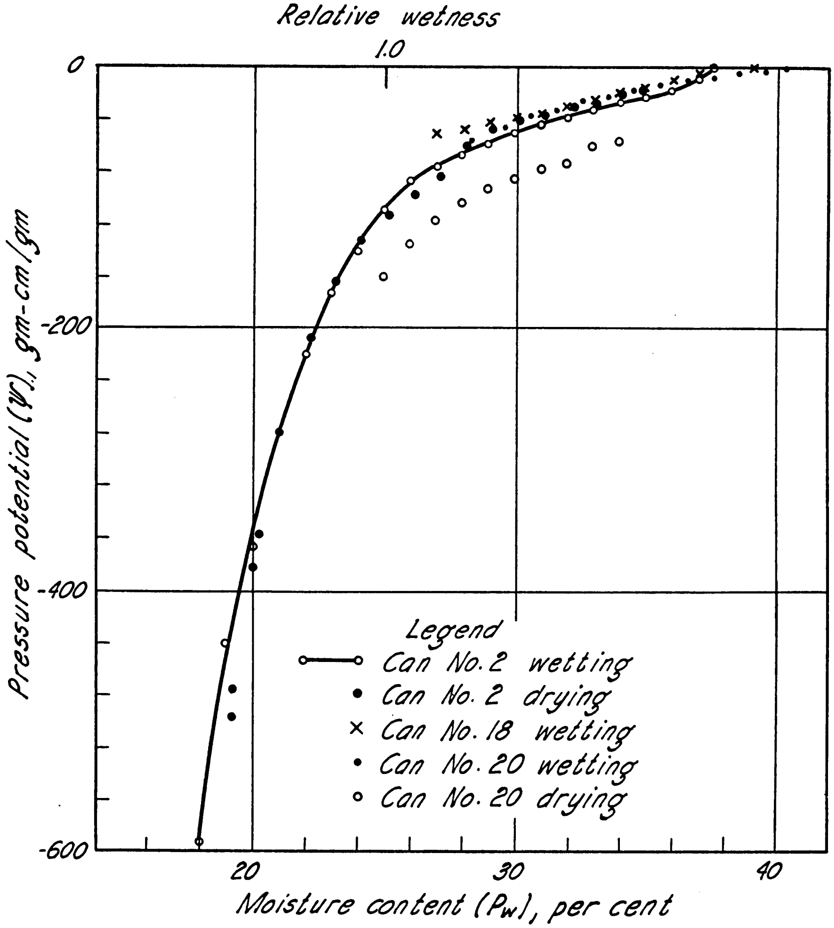

Fig. 16.—Curve of $\psi = f(P_w)$ for Yolo light clay wetting and drying.

of the soil column, then, would result in hysteresis, but opposite in sign to the hysteresis observed.

The differences between the wetting and drying pressure potential curves extend almost to saturation, the range of the negative radii of curvature as calculated from the pressure potentials and surface tension being from 14 to 50 microns. Within this range of moisture content, the solid particles must be entirely bathed with water, and probably no

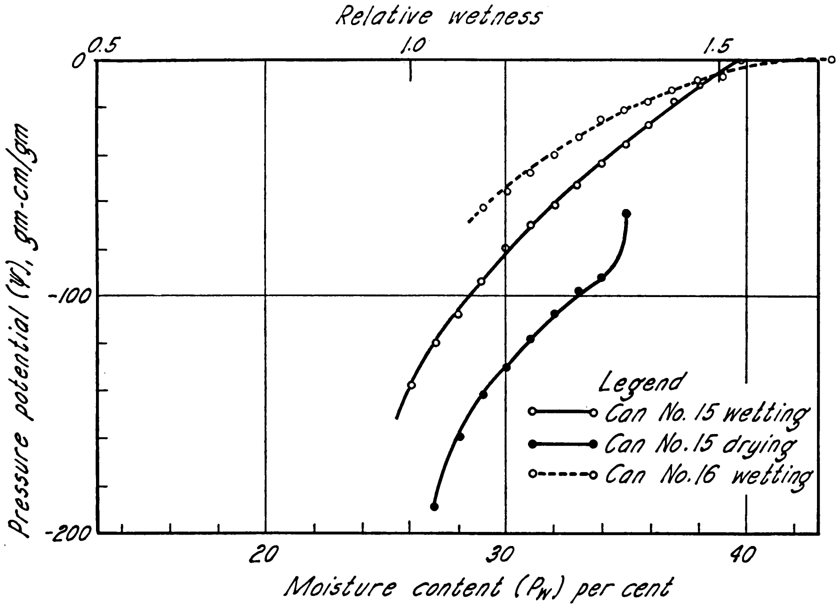

Fig. 17.—Curve of $\psi = f(P_w)$ for Yolo clay loam wetting and drying.

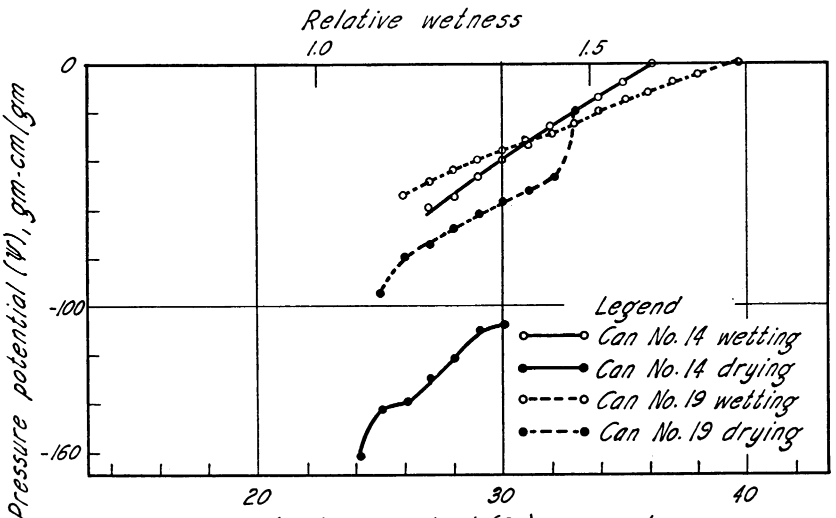

Fig. 18.—Curve of $\psi = f(P_w)$ for Yolo clay wetting and drying.

solid-air interface exists. Under such conditions, adsorbed air on the surface of the solid particles should play little or no part in the curvature of the water-air interface and resulting pressure potentials.

This investigation contributes no positive evidence as to the causative factors in hysteresis; however, the following enumeration of the conditions under which hysteresis was observed may contribute by limiting the field of conjecture as to these factors:

1. At a given negative pressure potential, soils held more water on drying than on wetting.

2. The calculated negative radii of curvature of menisci, within which range the principal hysteresis was observed, were 14 to 50 microns. Hysteresis may persist at radii much less than 14 microns, but under the experimental conditions imposed, drying did not proceed readily below that radius.

3. Soils settled and increased in apparent density as drainage progressed. If an increase in apparent density is the only significant structural change involved in shrinkage, then settlement would result in a higher rather than a lower pressure potential for a given moisture content.

4. As the soils dried, water flowed from the tensiometer cup to the soil. A lag in pressure equilibrium between the cup and the soil would result in a higher, rather than a lower, pressure potential for a given moisture content.

5. The magnitude of hysteresis increased as the range between the wetting moisture content and the drying moisture content increased, as indicated by the following data:

	Can No.	Per cent loss of water during drainage	Approximate hysteresis in gm–cm/gm
Yolo fine sandy loam	1	1	5 to 10
	17	5 to 12	10 to 20
Yolo light clay	2	2	+8 to —8
	20	4 to 6	40
Yolo loam	19	1 to 7	20
	14	5 to 8	70

It has been suggested that tensiometers installed in the soil would be a practicable means of charting the course of the soil moisture status through the relation of pressure potential to moisture content. The above data, however insufficient, indicate that the pressure potential may be not only dual-valued in terms of water content, but that the magnitude of the drying potential may depend upon the range through which the soil dried.

The Permeability of Soils to Water.—In slow motion such as that of water through soils, the velocity of flow, V, may be expressed as a product of the force acting to drive the water through the soil, and of a conductivity function, or the permeability of the soil to water, K. The mathematical expression of flow is given in the equation (*4*),

$$V = KF = -K\nabla(\psi + \omega + \lambda) = -K\nabla\Phi$$

where V represents the mean velocity of flow; F, proportional to V, is the total force per unit of mass acting to drive water through the soil

TABLE 4

Velocity of Flow of Water in the Soil Columns at Steady State

Soil type and can number		Distance from the water table to the surface of the soil column, centimeters	Depth of water transported to the surface	
			Centimeters×10^6 per second, V	Centimeters per day
Oakley sand, 3		105	0.23	0.02
Yolo sand, 13		42	0.52	0.04
Yolo fine sandy loam	1	105	0.37	0.03
	17	46	5.30	0.46
	20	42	5.60	0.48
Yolo clay loam	14	51	3.50	0.30
	19	50	5.50	0.47
Yolo light clay	2	105	0.87	0.08
	18	46	6.50	0.56
	20	43	7.10	0.61
Yolo clay	15	60	2.90	0.25
	16	50	5.30	0.46

and is composed of the gradients of pressure potential, ψ; the gravitational potential, ω; and the osmotic potential, λ. The permeability, K, is constant and independent of the rate of flow and the total potential gradient, $\nabla\Phi$.

In applying the general formula to the calculation of permeabilities in the soil columns, V (table 4) is expressed in centimeters per second, $F = -\nabla\Phi$ is expressed in grams per gram, and K has the dimensions of time. The gravitational potential gradient, $\nabla\psi$, is assumed to be constant and equal to one gram per gram. The osmotic potential, λ, is assumed to be constant and the osmotic potential gradient, $\nabla\lambda$, is therefore equal to zero. According to the above assumptions, and under the condition of this experiment in which all movement other than vertically upward or downward was eliminated, the total potential gradient in grams per gram may be written

$$\nabla\Phi = \nabla\psi + 1,$$

and since the pressure potential gradient at steady state was negative upwards

$$K = \frac{V}{-(\nabla\psi + 1)}.$$

The pressure potential gradient was evaluated at any desired points in the soil column by drawing tangents to the $\psi = f(H)$ curve for that column and determining their slope.

In this discussion of the permeability of soil to water, it is not intended to introduce new terms. In the interest of clarity, however, it is necessary to restate the definition of terms that will be frequently used:

Saturated permeability refers to the permeability of the soil when the soil is saturated with water. Saturated soil is a two-phase system, solid and liquid.

Unsaturated permeability is the permeability of the soil when it is unsaturated. Unsaturated soil is a three-phase system, solid, liquid, and gas. Unsaturated permeability is based on the flow of water through the soil in the vapor phase, or in the vapor and liquid phases.

Capillary permeability refers to liquid flow in unsaturated soil.

Vapor permeability refers to vapor flow in unsaturated soil.

The configuration of the moisture system, in soil at various degrees of unsaturation, has been amply discussed elsewhere in the literature; here, it is sufficient to say that vapor flow will take place in unsaturated soil at any total potential gradient other than zero. Capillary flow can take place only at those soil-moisture contents at which the water films are so connected as to allow liquid water to flow through water films from one position in the soil to another. *Continuous water films* are those which permit water, in the liquid phase, to flow through water films from one position in the soil to another. Water films are termed discontinuous when water in the liquid phase cannot flow through water films from one position in the soil to another. Continuous water films must be connected, but discontinuous water films may also be connected, the sole criterion for continuity, as here used, is that of flow as described above. If the soil moisture films are continuous, capillary flow will take place at any total potential gradient other than zero. If the soil moisture films are discontinuous, capillary flow is zero (*18*).

Permeability as a Function of Pressure Potential.—Soil permeability is measured per unit of cross-sectional area of soil. Since capillary flow takes place through moisture films, we would expect capillary permeability to increase with increasing effective cross section of moisture films, and hence with increasing moisture in the soil. In this study the moisture content has been expressed as a function of pressure potential, ψ, which is directly related to the vapor pressure of the soil moisture, and is an

TABLE 5*

WETTING AND DRYING POTENTIALS AND PERMEABILITY AS FUNCTIONS OF MOISTURE CONTENT; YOLO LIGHT CLAY, CAN No. 2

P_w	Wetting		Drying	
	ψ	$K\dagger\times 10^6$	P_w	ψ
18	−592	0.012	....	.....
19	−440	0.022	19.2	−476
20	−366	0.041	20.2	−358
21	−278	0.064	21.2	−280
22	−224	0.091	22.2	−208
23	−172	0.133	23.2	−162
24	−140	0.215	24.2	−126
25	−108	0.398	25.2	−111
26	− 86	0.795	26.2	− 98
27	− 76	0.88	27.2	− 82
28	− 67	0.97	28.2	− 60
29	− 58	1.06	29.2	− 48
30	− 50	1.21	30.2	− 41
31	− 44	1.48	31.2	− 36
32	− 37	1.91	32.2	− 31
33	− 32	2.56	33.2	− 28
34	− 27	3.30	34.2	− 23
35	− 22	4.40	34.9	− 16
36	− 16	6.15	....	.....
37	− 8	8.60	....	.....
37.5	0	12.3	....	.....

* Owing to the limitations of space in this paper, tabular experimental data on the distribution of pressure potentials and moisture is given for one soil column only.

† Permeability, K, was calculated from the velocity of flow, V, expressed in centimeters per second and the pressure potential gradient, $\nabla\psi$, expressed in grams per gram. The values for V were taken from table 4, and the values for $\nabla\psi$ were taken as the slope of the curve of $\psi=F(H)$ in figure 11.

especially useful function of the soil moisture density because it is also an index of its configuration. Accordingly, unsaturated permeability will be investigated as a function of ψ (table 5 and figs. 19, 20).

Permeability is maximum at, or near, a pressure potential of zero for all the soils covered by this experiment. The permeability remains constant from zero pressure potential down to pressure potentials of — 10 to — 40. Saturation persists for some distance above the plane of zero-pressure potential, but this distance could not be determined by the method used for taking moisture samples. This height was probably from 1 to 3 centimeters above the plane of zero-pressure potential, and

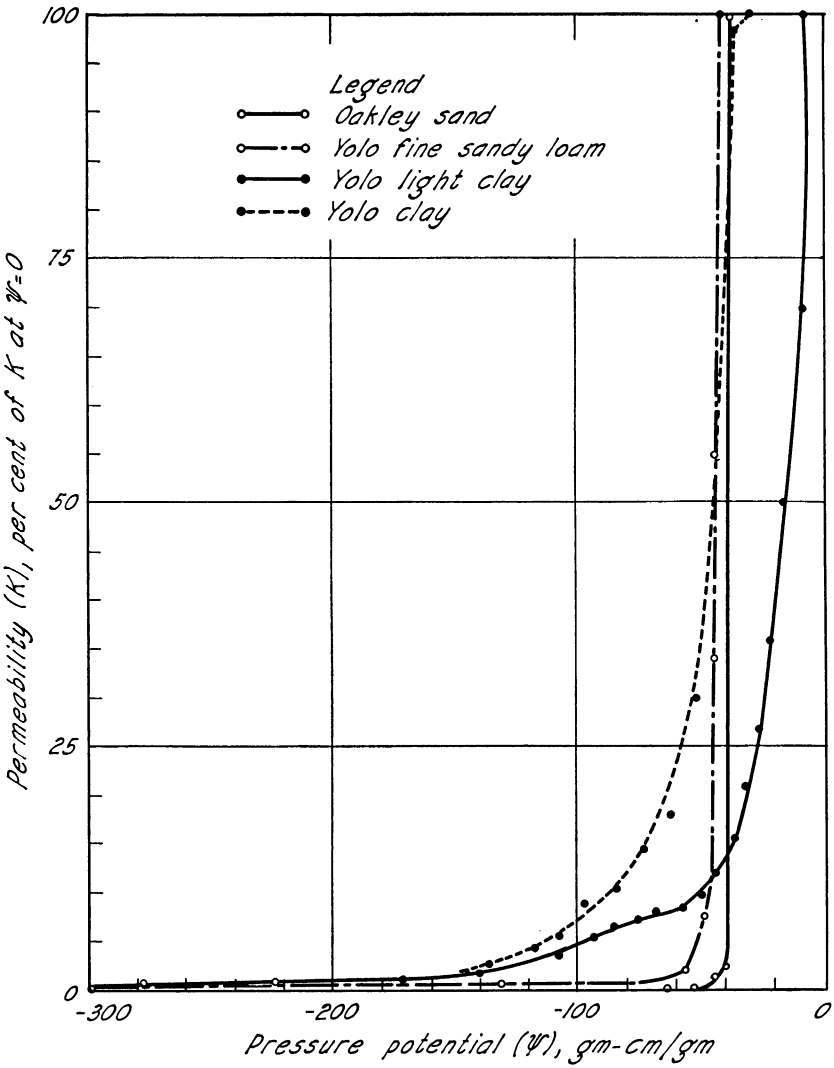

Fig. 19.—Permeability as a function of pressure potential, $K = f(\psi)$ with permeability expressed as a percentage of the permeability at a pressure potential of zero.

was entirely too small to account for the high permeability extending 20 to 30 centimeters above the piezometric surface.

Permeability of the Yolo clay was less in the range of positive pressure than that at pressure potentials of zero to —40 gm–cm/gm. Under certain conditions differential swelling of soil colloids effected by wetting at

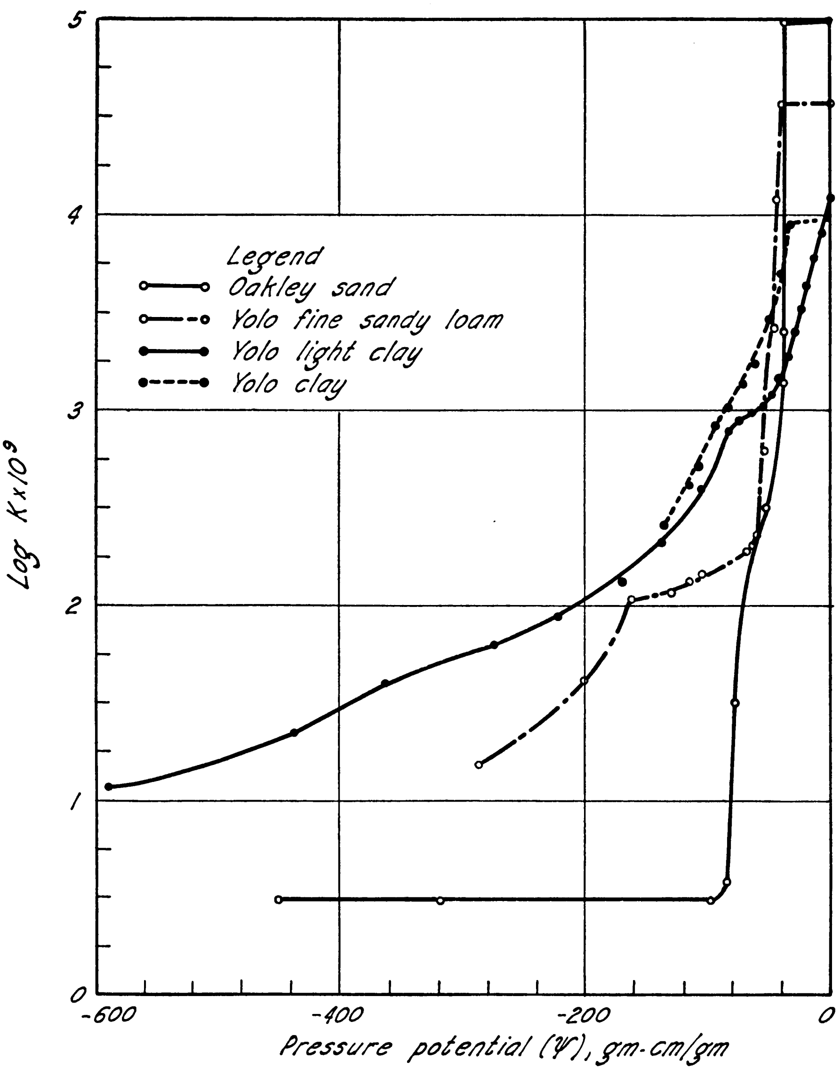

Fig. 20.—The logarithm of the permeability times 10^9 as a function of the pressure potential, $\log (K \times 10^9) = f(\psi)$, plotted for four soils. $K = -\frac{V}{\nabla\Phi}$, in which V is expressed in cubic centimeters per second, and $\nabla\Phi$ in grams per gram.

different pressure potentials may result in a greater permeability above the piezometric surface than that in the range of positive pressure. Yolo clay swells on wetting, but no change in the over-all volume of the soil was detected in the cans. In such swelling the solid particle with its absorbed water may act as a larger solid particle, as far as the permeability of the swollen soil is concerned. This would result in a greater effective volume of solid and lesser effective volume of pore space per unit volume of soil, and likewise, a lower total effective pore area and fewer continuous pores per unit of cross-sectional area of the soil column. If the soil colloids swell in proportion to the pressure potential at which they are wetted, the total pore space effective in the conduction of water in the soil columns would decrease as this potential increased. Hence the per cent of effective pore space in the range of positive potentials would be less than in the range of negative potentials, and permeability may be greater for some distance above the piezometric surface than that obtained below this surface.

The Effect of Texture on Soil Permeability.—The effect of texture on the manner with which permeability changes with pressure potential is shown in figures 19 and 20. For the soils studied, saturated permeability increases with increasing coarseness of texture. In the range of capillary flow, the rate of change of permeability with pressure potential, $\partial K/\partial \psi$, increases with increasing coarseness of texture, such as to produce the reversal of permeabilities shown in figure 20. The soils arranged in permeability series are, at saturation:

$$\text{sand} > \text{fine sandy loam} > \text{light clay} > \text{clay}$$

and at $\psi = -100$

$$\text{sand} < \text{fine sandy loam} < \text{light clay} < \text{clay}.$$

Zero Capillary Permeability.—The evaluation of the soil moisture content, or the pressure potential in the soil at which capillary conductivity becomes zero, is of importance in the study of soil-moisture problems, such as: the distribution of water in the soil, the translocation of soluble salts, the maximum height of capillary rise, etc. Richards (*18*) states that the water in soils is no longer present in a continuous liquid phase, and capillary flow ceases at the point where capillary conductivity becomes zero. At field capacity or at the normal moisture capacity the capillary permeability of soils must be zero or approximately zero and any water translocation must take place in the vapor phase (*13, 22, 33, 34*).

In this paper zero capillary permeability is discussed under the two criteria: the pressure potential of the wetting front, and the pressure potential at which $\partial K/\partial \psi = 0$.

The advance of the wetting front was observed in the soil columns through celluloid-covered holes in the soil cans. Core moisture samples were taken at the wetting front with a $\frac{1}{4}$-inch cork borer, care being taken to include no dry soil. The center of the core was about $\frac{3}{16}$-inch below the wetting front. Since there was a moisture gradient in the soil column with the moisture density increasing with distance below the front, the samples may show a higher moisture content than that of the wetting front. The increase in the experimental value for moisture content due to a moisture gradient could not be determined because the gradient itself could not be evaluated. The moisture gradient, however, decreases with increasing height of rise; and if the effect of the moisture

TABLE 6

MOISTURE CONTENT AT WETTING FRONT FOR THREE YOLO SOILS

Fine sandy loam, can No. 17		Light clay, can No. 20		Clay, can No. 16	
Elevation of sample	P_w	Elevation of sample	P_w	Elevation of sample	P_w
cm	*per cent*	*cm*	*per cent*	*cm*	*per cent*
13.1	19.9	7.6	24.6	19.9	26.1
20.4	19.6	10.3	25.1	30.0	26.8
23.2	20.2	27.6	24.3	40.1	24.9
27.9	21.0	35.2	24.0	50.3	25.9
33.4	20.5	37.8	24.4	70.5	25.6
35.9	20.8	40.5	24.1	....	....
40.6	21.6	50.5	25.9	....	....
50.7	19.8	....	....	....	....
70.9	20.6	....	....	....	....
81.1	19.7	....	....	....	....
Mean P_w (per cent)	20.4	....	24.6	....	25.9
ψ (gm–cm/gm)*	−92	....	−120	....	−140

* ψ values taken from $\psi = f(P_w)$ curves.

gradient is appreciable, the moisture content of the wetting front samples should decrease from the bottom of the soil column to the top. No such relation was found; the wetting front samples showed a relatively uniform moisture content throughout the length of the soil columns. Table 6 lists wetting front moisture contents with the elevation of the front above the base of the soil columns.

Wetting front samples were not taken from the Oakley sand; but from the nature of its curve of $\psi = f(P_w)$ it is assumed to be at a pressure potential of approximately — 80 gm–cm/gm, and a moisture content of 5.0 per cent.

The following experimental observations, along with certain theoretical considerations, may aid in characterizing the wetting front:

1. Water advances in a front from wet to drier soil under the influence of capillarity (*14, 36*). Beyond the front, the soil remains apparently dry, and immediately at and behind the front, the soil is apparently

completely wetted. Macroscopically, there is a sharp line of demarcation between the obviously wet soil and the obviously dry soil.

2. The moisture content of the wetting front determined by sampling is constant, indicating a constant potential and a constant radius of curvature. The pressure potential of the wetting front ranged from — 80 gm–cm/gm for the Oakley sand to — 140 gm–cm/gm for the Yolo clay with intermediate values for soils of intermediate texture.

3. The moisture content of the dry soil immediately beyond the wetting front was not definitely known. The air-dry soil was in equilibrium with air at a relative humidity of approximately 42 when wetting began. As the first approximation we may assume a relative humidity of 50 at a distance of 1 mm beyond the wetting front making the pressure potential gradient across this region 1×10^7 gm/gm. These assumptions may be in appreciable error, but whatever logical values are assumed, the pressure potential gradient from the dry soil to the wet is obviously very great.

4. The existence of a great pressure potential gradient from the dry soil to the wetting front should insure the maintenance of the lowest possible pressure potential, and hence, the thinnest possible moisture films at the front consistent with continuous moisture films behind the front.

5. We may adapt the explanation given by Adam (*1*) for the rise of water in capillary tubes to the rise of water by capillarity through a porous medium such as soil, although it is recognized that the capillary tube is filled with water back of the advancing meniscus, and in unsaturated soil the water films are only partly bounded by a solid.

A. The liquid is not pulled through the soil by a hypothetical tension acting on the film which clings to and climbs up the surface of the soil particles.
B. The energy relations determine what the stable contact angle shall be.
C. The fluidity of the liquid permits the molecules to move about until they generate that angle.
D. The contact angle and the dimensions and shape of the voids between the solid particles, determined by the effective texture and packing arrangement, govern the curvature of the liquid-air interface.
E. The pressure difference arises from the free energy resident in the liquid-air interface.
F. The liquid then flows up under the hydrostatic pressure.

Disregarding for the present the translocation of water through soil in the vapor phase and the possibility of the establishment of continuous moisture films through the agency of vapor flow, we may characterize the wetting front and some of its relations to the soil-moisture system in general from the five preceding observations:

1. The wetting front represents an irregular surface of discontinuity with continuous moisture films behind the front, and discontinuous or nonexistent films beyond the front.

2. At moisture contents below that characteristic for the wetting front, the capillary permeability of a soil to water in the liquid phase is zero. At these lower moisture contents the films are discontinuous, and there is no mechanism for liquid flow.

3. The magnitude of the pressure potential gradient from the dry soil to the wetting front has no influence on the rate of advance of this front except that a wetter soil requires less water to establish continuous films than a drier soil. The advance of the wetting front is by liquid flow, and is proportional to the pressure potential gradient back of the wetting front. The water flows under hydrostatic pressure.

4. At a given temperature, the curvature of the moisture films at the wetting front is characteristic for the soil solution and the soil, and does not vary with elevation of rise.

5. The moisture content at the wetting front is constant for a given soil solution and soil.

6. At constant temperature, the pressure potential at the wetting front is constant for a given soil solution and soil.

7. Water cannot rise by capillarity beyond the elevation at which the sum of the gravitational potential, the osmotic potential, and the pressure *potential characteristic of the wetting front* is equal to zero.

All the considerations thus far with reference to the wetting front have concerned only liquid flow through soils without the necessary intervention of vapor flow which is always present in a three-phase system. The soil has also been considered as a granular solid of constant effective texture and structure. The changes in the effective texture and structure with wetting cannot be completely described. It is known, however, that the mass effect of these changes is relatively insignificant in coarse-textured soil, but may be of considerable magnitude in other soils. Swelling of the colloidal fraction due to wetting is the only change in the solid phase that will be considered.

With the wetting front advancing rather rapidly through air-dry soil, the structure and effective texture immediately beyond the wetting front is probably very much the same as that which is characteristic for the dry soil. When the wetting front approaches its maximum height above the water table and advances more slowly, wetting of the soil in advance of the front through the agency of vapor flow is of greater relative magnitude, the soil colloids swell, a lesser radius of curvature of the liquid surface may establish continuous moisture films, and the pressure potential of the wetting front may decrease progressively as the front advances from the water table to the maximum height of capillary rise. Experimental evidence is not at hand to permit a quantitative evaluation of the factors in the above speculation. For the present it seems worth while to bear these factors in mind, although they have not been determined, and though eventually they may be found to be of little significance.

Unsaturated permeability cannot be separated experimentally into its components of vapor and liquid permeability. If, however, we assume that vapor permeability for a given soil is constant when liquid permeability is zero, then liquid permeability would be zero when $\partial K / \partial \psi = 0$. In figure 19 the permeability of four soils is plotted as a function of the pressure potential. The permeability at each potential is expressed as a percentage of the permeability at zero pressure potential. The values for the pressure potentials at which capillary permeability becomes zero, as determined from moisture samples taken at the wetting front, are: Yolo fine sandy loam, — 92 gm–cm/gm; Yolo light clay, — 120 gm–cm/gm; and Yolo clay, — 140 gm–cm/gm. These potentials referred to the curves of $K = f(\psi)$, however, are not at values of ψ at which $\partial K / \partial \psi = 0$. But below these potentials both K and $\partial K / \partial \psi$ are very small. It is indicated that the potential at the wetting front represents, at least to the first approximation, the potential below which discontinuity occurs in the soil-moisture system, and is a critical point on the permeability curve at which capillary permeability becomes approximately zero. It is also indicated that the determination of the wetting front potential by sampling for moisture content is a practicable experimental procedure. This is worthy of further investigation.

INTERPRETATION OF SOME SOIL MOISTURE PHENOMENA IN TERMS OF PERMEABILITY

The Moisture Equivalent.—The moisture equivalent has been considered as representing a point on the pressure potential curve at which the pressure potential gradient of the soil is in approximate equilibrium with the centrifugal force applied, or at which the pressure potential is equal to —1000 gm–cm/gm (*21*). According to the data presented in this paper, the pressure potential at the moisture equivalent is much greater than — 1000 gm–cm/gm, varies with the texture of the soil, and represents the approximate ψ on the $K = f(\psi)$ curves at which the water in the soil becomes discontinuous, and the capillary permeability becomes zero.

Vapor permeability is high in sands. In centrifuging, the combined vapor and liquid flow reduces the moisture content of sand in the centrifuge cup to a pressure potential below that at which capillary flow ceases. In heavy clay the vapor permeability is low. The combined vapor and liquid flow is not sufficient to reduce the pressure potential of heavy clay to the point at which capillary flow ceases. The fact that the moisture equivalent of clay is generally higher, and of sands is generally lower than the field capacity would be expected from the above considerations of permeability.

Hysteresis of Curves of $pF = f(P_w)$.—An adaptation of a technique originally proposed by Bouyoucos (*5*) has been used for the derivation of data for the development of $\mathrm{pF} = f(P_w)$ curves. The equipment required in this technique is: a source of vacuum, a Büchner flask, and filter paper coated with a thin layer of silt. The silt-coated paper forms a porous plate of small pore dimension. To determine the drying pF, a thin layer of soil is placed on the filter paper, and a continuous liquid phase is established extending through the filter plate, funnel, and stem, and into the filter flask. A constant vacuum is applied to the flask for a time considered sufficient to remove excess water. At the end of the drying time the soil is removed from the filter and the moisture content determined. The pF at that moisture content is assumed to be equal to the logarithm of the negative pressure applied. A drying curve of $\mathrm{pF} = f(P_w)$ is developed from values of pF and P_w derived by repeating the procedure at different suction pressures. The technique for deriving the wetting pF is the reverse of that used in drying. In wetting, air-dry soil takes up water against a constant negative pressure maintained in the continuous liquid phase.

The assumptions necessary for the application of pF data derived by the above technique are:

1. At the end of the wetting or drying time, the pressure in the soil moisture films is at approximate equilibrium with the negative pressure applied.

2. The moisture films are continuous from the water in the flask through the soil layer.

The first assumption can only be valid within that moisture range in which the second assumption is true, since this technique is an approximate and rapid method for determining pF, and is applicable only if water transfer can take place in the liquid phase. The time allowed for each determination is obviously too short to allow establishment of equilibrium moisture conditions through the agency of vapor flow.

The above-described technique, used at pressure potentials below which capillary permeability equals zero, would give erroneous results. On drying, the soil would lose water readily down to the pF at which the capillary permeability becomes zero. Further loss of water would be very slow through the agency of vapor flow. The experimental drying moisture content and pF would be higher than the true values representing equilibrium with the suction applied. On wetting, no capillary flow could take place, and the soil would receive water only by condensation of water vapor. The experimental wetting moisture content and pF would be lower than the true values representing equilibrium with the suction applied.

Curves of pF $= f(P_w)$ derived by the above technique show hysteresis of considerable magnitude between the wetting and drying curves. At a given pF the moisture content in the drying curve is much higher than that in the wetting curve. It is suggested that many of the data were secured in the moisture range in which the moisture films were discontinuous and the capillary permeability was zero; and that approximate pressure equilibrium was not established between the soil water and the water in the filter pores.

Moisture Distribution in Stratified Soils.—It is a well-known fact that a heavier-textured soil, underlaid by a coarse-textured soil, has a higher field capacity than the unstratified heavier soil (*2*). This phenomenon can be explained on the basis of the characteristic pressure potential for each soil at which capillary permeability becomes zero. To illustrate this point, let us consider two columns of soil as follows:

1. Column of unstratified Yolo clay
   - A. K is approximately zero at $\psi = -140$
   - B. $P_w = 26$ per cent at $\psi = -140$.
2. Column of Yolo clay stratified with Oakley sand; K of Oakley sand is approximately zero at $\psi = -80$.

After irrigation of the unstratified Yolo clay, water will flow downward under the influence of gravity until the moisture films become discontinuous. The final moisture distribution in the soil, neglecting vapor flow and in the absence of a water table, would be at $\psi = -140$ and $P_w = 26$ per cent.

After irrigation of the stratified column, water will flow downward through the clay with a pressure potential at the wetting front of approximately — 140. When the wetting front reaches the sand, flow cannot take place until the potential in the clay becomes greater than — 80 which is the minimum pressure potential at which flow is possible in the sand. (For Yolo clay $P_\omega = 30$ at $\psi = -80$.) The equilibrium moisture distribution in the clay, neglecting vapor flow, will be:

Distance above sand in centimeters	ψ	P_w
0	—80	30
0 to 60	—80 to —140	30 to 26
Above 60	—140	26

If we assume the same two soil columns, ideally, under conditions of capillary rise:

1. With the top of the sand stratum less than 80 centimeters above the water table, the height of capillary rise will not be affected. At equilibrium, capillary water will rise to 140 centimeters above the water table.
2. If the bottom of the sand stratum is at any elevation between 80 to 140 centimeters above the water table, capillary rise will stop at 80 centimeters or at the bottom of the sand stratum.
3. If the sand stratum occurs so that a point 80 centimeters above the water is in sand, then capillary rise will reach its maximum in the sand at 80 centimeters above the water table. Theoretically, a shift of a few millimeters in the elevation of the sand stratum may make a difference of 60 centimeters in the maximum height of capillary rise.

SUMMARY

Data on the permeability of soils to water under saturated conditions is abundant; however, the unsaturated permeability of soils has received relatively little study, and published data on the subject are meager. The introduction of the potential function gave rise to the dynamic method in the study of unsaturated flow, and the development of the tensiometer instrument has made possible the direct determination of pressure potentials.

All published data now available on the permeability of soil to water in unsaturated flow were derived by the dynamic method from pressure potentials determined directly from tensiometers placed in the soil. This method was used in the soil-permeability studies reported in this paper.

Six soils, ranging in texture from sand to clay, were investigated under laboratory conditions of capillary rise. The soils were placed in metal cylinders with water supplied to their bases at a constant pressure sufficient to establish saturated conditions in the lower portion of the columns. Water flowed upward through the columns under the influence

of positive hydrostatic pressures in the saturated zone, and of negative hydrostatic pressures, or by capillarity, from the water table to the surface of the columns where it was removed by evaporation.

Pressure potentials in the unsaturated soil were studied as functions of moisture contents by determining the pressure potentials, ψ in gram-centimeters per gram, directly from tensiometer readings and the moisture contents, P_w, by sampling the soil columns. The relation between ψ and P_w for each soil was represented graphically in curves of $\psi = f(P_w)$. Hysteresis in the relation of ψ to P_w was found for all the soils, according to whether they were wetting or drying. At a given P_w, ψ was less after drainage than during the wetting process. The data of this experiment also indicate that for soils drying, the pressure potential depends upon the range through which the soil has dried.

The pressure potential in an unsaturated soil at constant moisture content increases with increasing temperature, and the amount of water held in the soil at a given pressure potential decreases with increasing temperature. During periods of temperature change in a soil column in which there is a high water table, these relations cause wide variations in the rate of water uptake from a water table. Under field conditions, rapid changes in soil temperature above a water table would be accompanied by rising water tables with rising temperature, and falling water tables with falling temperature.

The pressure potential of the water films in a soil is a measure of the curvature of the films and an index of the degree to which the soil is saturated. The relation of soil permeability, K, to pressure potential was studied and curves of $K = f(\psi)$ were developed. K could also be studied as a function of P_w through the relationship between ψ and P_w. Permeability was a maximum at or near saturation and decreased rapidly with decreasing P_w to approximately the moisture equivalent of the soil, at which moisture content the permeability was very low and remained constant or decreased only slightly with further decreases in moisture content. At this point $\partial K / \partial \psi = 0$ (approximately). This moisture content is also approximately that of the wetted front generated as the water advanced upward through the dry soil above a water table. These two criteria, the P_w at which $\partial K / \partial \psi = 0$ and the P_w of the wetting front, are interpreted as representing the P_w at which the moisture films in the soil become discontinuous and at which the capillary permeability of the soil is zero.

The texture of a soil affects permeability by its influence on the size, number, and continuity of the interspaces or pores. For soils of a like nature, such as the members of a single soil series, the size of pores decreases and the number of pores increases with increasing fineness of texture. The soils used in this experiment, arranged in order of permeability are, for saturated flow

sand > fine sandy loam > light clay > clay

and for unsaturated flow at $\psi = -100$

sand < fine sandy loam < light clay < clay.

If arranged in order of decreasing pressure potential at which unsaturated flow is approximately zero, the sequence obtained is:

sand > fine sandy loam > light clay > clay.

Knowledge of the variation of permeability with texture, especially the pressure potential at which capillary permeability is approximately zero, is fundamental to the consideration of the relative rates and maximum height of capillary rise, to the field capacity in stratified and nonstratified soils, and to single-valued "constants" such as the moisture equivalent, the field capacity, and the normal moisture-holding capacity. These experiments indicate that the pressure potential of the soil moisture at these constants varies with the texture of the soil. They are at the approximate ψ on the curves of $K = f(\psi)$ at which the moisture films in the soil become discontinuous and the capillary permeability becomes zero.

ACKNOWLEDGMENT

The author wishes to acknowledge his indebtedness for advice and helpful criticism to Dr. G. B. Bodman under whose direction the investigations reported herein were carried out.

LITERATURE CITED

1. ADAM, N. K.
1930. The physics and chemistry of surfaces. 332 p. Oxford University Press.

2. ALWAY, F. J., and G. R. MCDOLE.
1917. Relation of the water retaining capacity of a soil to its hygroscopic coefficient. Jour. Agr. Research **9**:27–71.

3. BODMAN, G. B., and N. E. EDLEFSEN.
1933. Field measurement of the permeability to water of a silt loam soil at University Farm, Davis, California. *In:* Abstracts of Papers Presented at the Meeting of the Western Society of Soil Science at Salt Lake City, Utah. 6 p. (Mimeo.)

4. BODMAN, G. B., and N. E. EDLEFSEN.
1934. The soil moisture system. Soil Sci. **38**:425–44.

5. BOUYOUCOS, J. G.
1929. A new, simple, and rapid method for determining the moisture equivalent of soils. Soil Sci. **27**:233–40.

6. BUCKINGHAM, E.
1907. Studies on the movement of soil moisture. U. S. Dept. Agr. Bur. Soils Bul. **38**:1–61.

7. GARDNER, W.
1919. The movement of moisture in soil by capillarity. Soil Sci. **7**:313–18.

8. GARDNER, W.
1920. Capillary transmission constant and methods of determining it experimentally. Soil Sci. **10**:103–26.

9. GARDNER, W., O. W. ISRAELSEN, N. E. EDLEFSEN, and N. S. CLYDE.
1922. The capillary potential function and its relation to irrigation practice. Soil Sci. **11**:215–32.

10. GREEN, HEBER.
1911. The flow of air and water through soils. Jour. Agr. Research **4**:1–24.

11. HAINES, W. B.
1930. On the existence of two equilibrium series in soil capillarity phenomena. Proc. and Papers of the Second Internatl. Cong. Soil Sci. **1**:8–14.

12. HAINES, W. B.
1930. Studies on physical properties of soils: V. The hysteresis effect in capillary properties and modes of distribution associated therewith. Jour. Agr. Sci. **20**:98–116.

13. KEEN, B. A.
1927. The limited role of capillarity in supplying water to plant roots. Proc. and Papers of the First Internatl. Cong. Soil Sci. **1**:504–12. Comn. I.

14. MCLAUGHLIN, W. W.
1920. Capillary movement of soil moisture. U. S. Dept. Agr. Bul. **835**:1–70.

15. MCLAUGHLIN, W. W.
1924. The capillary distribution of moisture in soil columns of small cross section. U. S. Dept. Agr. Bul. **1221**:1–22.

16. RICHARDS, L. A.
1928. The usefulness of capillary potential to soil-moisture and plant investigations. Jour. Agr. Research **37**:719–42.

17. RICHARDS, L. A.
1932. Capillary conduction of liquids through porous mediums. Physics **1**: 318–34.

18. Richards, L. A.
1936. Capillary-conductivity data for three soils. Jour. Amer. Soc. Agron. **28**: 297–300.
19. Richards, L. A.
1936. Tensiometers for measuring the capillary tension of soil water. Jour. Amer. Soc. Agron. **28**:352–58.
20. Richards, L. A., and B. D. Wilson.
1936. Capillary conductivity measurements in peat soils. Jour. Amer. Soc. Agron. **28**:427–31.
21. Schofield, R. K.
1935. The pF of water in soil. Trans. Third Internatl. Cong. Soil Sci. **2**:37–48.
22. Shaw, C. F.
1927. The normal moisture capacity of soils. Soil Sci. **23**:303–17.
23. Shaw, C. F., and A. Smith.
1927. Maximum height of capillary rise starting with soil at capillary saturation. Hilgardia **2**(11):399–409.
24. Slichter, C. S.
1898. Theoretical investigation of the motions of ground water. U. S. Geol. Survey, 19th Ann. Rept. Part **2**:301–84.
25. Smith, A.
1927. Effect of mulches on soil temperature during the warmest week in July, 1925. Hilgardia **2**(10):385–97.
26. Smith, A.
1929. Daily and seasonal air and soil temperatures at Davis, California. Hilgardia **4**(3):77–112.
27. Smith, A.
1929. Comparison of daytime and nighttime soil and air temperatures. Hilgardia **4**(10):241–72.
28. Smith, W. O.
1932. Capillary flow through an ideal uniform soil. Physics **3**:139–47.
29. Smith, W. O.
1933. Minimum capillary rise in an ideal uniform soil. Physics **4**:184–93.
30. Smith, W. O.
1933. Final distribution of retained liquid in an ideal uniform soil. Physics **4**:428–38.
31. Smith, W. O., P. D. Foote, and P. F. Busang.
1931. Capillary rise in sands of uniform spherical grains. Physics **1**:18–26.
32. Van Bemmelen, J. M.
1910. Die Adsorption. 548 p. T. Steinkopff. Dresden.
33. Veihmeyer, F. J., and A. H. Hendrickson.
1927. Soil moisture conditions in relation to plant growth. Plant Physiol. **2**:71–82.
34. Veihmeyer, F. J., and A. H. Hendrickson.
1931. The moisture equivalent as a measure of field capacity. Soil Sci. **32**:181–93.
35. Wadsworth, H. A.
1931. Further observations upon the nature of capillary rise through soils. Soil Sci. **32**:417–34.
36. Wadsworth, H. A., and A. Smith.
1926. Some observations upon the effect of the size of the container upon the capillary rise of water through soil columns. Soil Sci. **22**:199–211.